■ ✦ **Environment
Canada**

**Environnement
Canada**

**Canada
Centre
For Inland
Waters**

**Centre
Canadien
Des Eaux
Intérieures**

DEVELOPMENT AND EVALUATION OF AN EXPERIM

FRAZIL ICE MEASUREMENT INSTRUMENT

by

Gee Tsang

UNPUBLISHED REPORT

RAPPORT NON PUBLIE

This manuscript has been submitted to

Department of Fisheries and the Environment, Inland Waters Directorate

for publication in its Scientific Series

and the contents are subject to change.

This copy is to provide information

prior to publication.

DEVELOPMENT AND EVALUATION OF AN EXPERIMENTAL

FRAZIL ICE MEASUREMENT INSTRUMENT

by

Gee Tsang

Hydraulics Section

Hydraulics Research Division

Canada Centre for Inland Waters

December, 1976

ABSTRACT

Theoretical investigations show that the presence of frazil ice in water can be quantitatively measured by its effect on the conductivity and the permitivity of the water. At frequencies much lower than 10^7 Hz, the conductivity effect of frazil ice predominates and at frequencies much higher than 10^7, the ice effect on permitivity is predominant. An experimental instrument based on the resistance (i.e. conductivity) principle has been constructed and tested. Experiments were performed in a cold room with frazil ice produced in a beaker. The experiments showed that the laboratory instrument could quantitatively sense the presence of ice. The detailed circuit of the experimental instrument is shown. Some modifications of the circuit and the probe for improving the instrument are suggested as a consequence of the laboratory experiments and further theoretical investigations. The concentrations of frazil ice measured by the experimental instrument were by average about three times the concentration calculated theoretically. If the frazil ice crystals are assumed to have elongated spheroidal shapes with a length to breadth ratio of 10:1, the measured concentrations were about twice the calculated concentration. Further theoretical investigation is needed to explain the above puzzle. This puzzle, however, is a welcome one because it increases the sensitivity of the instrument.

The work report herein is the phase I part of an instrument development project. The design and production of an improved and manufacturable instrument will be the phase II of the project.

RESUME

Des études théoriques indiquent que la présence de cristaux de
glace dans l'eau peut se mesurer quantitativement par leurs effets sur
la conductivité et la constante diélectrique de l'eau. A des fréquences
bien inférieures à 10^7 Hz l'effet de conductivité des cristaux de
glace prédomine, tandis qu'à des fréquences bien supérieures à 10^7 Hz,
c'est l'effet de la glace sur la constante diélectrique qui prédomine.
Un instrument expérimental, fondé sur le principe de résistance
(conductivité) a été fabriqué et mis à l'essai. Les expériences ont
eu lieu dans une pièce froide, et les cristaux de glace ont été produits
dans un vase à bec. Les expériences ont démontré que l'instrument de
laboratoire pouvait détecter quantitativement la présence de la glace.
Le circuit détaillé de l'instrument expérimental figure dans le présent
rapport. Par suite des expériences de laboratoire et d'autres études
théoriques, certaines modifications du circuit et de la sonde sont pro-
posées pour améliorer l'instrument. Les concentrations de cristaux de
glace mesurées par l'instrument expérimental ont représenté en moyenne le
triple de la concentration calculée théoriquement. Si l'on présume que
les cristaux de glace ont une forme sphéroïdale allongée et que la pro-
portion entre leur longueur et leur largeur est de 10 contre 1, les
concentrations mesurées ont représenté environ le couble de la concen-
tration calculée. Une autre étude théorique s'impose pour expliquer
l'énigme ci-dessus. Toutefois, celle-ci est opportune car elle démontre
la sensibilité de l'instrument.

Le présent rapport constitue la première phase d'un projet de création d'un instrument. La conception et la production d'un instrument amélioré pouvant être fabriqué en série feront l'objet de la deuxième phase du projet.

TABLE OF CONTENTS

INTRODUCTION

Recently, noticeable progress has been made in many areas of ice research. Advances made on frazil ice research, however, remained limited because of, to a large extent, the lack of a working instrument which can quantitatively measure frazil ice.

Efforts, however, have been made either in devising a technique to calculate the quantity of frazil ice or in developing an instrument to measure frazil ice concentration. Kristinsson (1970) measured the resistance between two wires wound spirally on an insulated rod immersed in frazil ice-laden water and correlated the resistance to the average frazil ice concentration over the rod's depth. Gilfilian et al (1972) calculated the quantity of frazil ice formed in a river from the measured change in conductivity of the water, before and after ice formation. Kristinsson's instrument was crude and developed mainly empirically. The development was not under a rigid theoretical guidance and lacked analytical refinement. No attempt was made by Gilfilian et al to develop an instrument from their technique. The conceptual design of an instrument for sensing the frazil ice concentration, the velocity of the frazil ice and the velocity of the flowing water was proposed by Tsang (1973). The design is based on the same conductivity principle used by Kristinsson. Theoretical ground work was laid to guide the design. An instrument based on laser principles was developed by Schmidt and Glover (1975). From the scattering of a laser beam by frazil ice crystals, the concentration of frazil ice

and the velocity of the ice crystals were measured. The instrument cannot be considered as successful, despite its high cost and complexity; it only gave accurate measurements at the early stage of ice formation and when the frazil ice concentration is low.

The work report herein is the further development of Tsang's earlier conceptual instrument. The development is on the frazil ice measurement component of the instrument. The theoretical work is expanded to the effect of frazil ice on the impedance of the water, instead of on conductance alone. Criteria are established to guide the design of a functional instrument for measuring frazil ice. An experimental instrument was constructed and its laboratory testing showed great promise and encouragement. Further refinement of the instrument, which is presently being undertaken, should produce a much needed instrument for fast and accurate frazil ice measurement at a low cost.

THEORY

Although pure water is electrically non-conductive, natural water is conductive because of mineral contents. Natural water from different sources may have different conductivity because of different mineral contents. In southern Ontario, the typical conductivity of natural water is of the order of 0.05 S/m $(ohm-m)^{-1}$. As ice is formed from water, impurities are rejected. Ice, therefore, may be considered non-conductive. From measuring the change of conductivity in water, the presence and quantity of frazil ice may thus be detected.

The dielectric constant of ice is also different from that of water. In addition, it is frequency dependent. At low frequencies, the relative dielectric constant of ice is close to that of water, at about 80. As the frequency increases, the dielectric constant of ice decreases. At 100 KHz, the relative dielectric constant of ice drops to about 5, while that of water remains the same at 80. Thus, the concentration of frazil ice in water may also be measured by sensing the change in the dielectric constant in water.

The immersion of two plates in water gives the equivalent electrical circuit of a resistance and a capacitance connected in parallel. The immersion of three plates in water, with the middle plate common to both side plates (See Fig. 1), gives two such equivalent circuits. If ice is allowed to enter one pair of plates (probe x) and excluded from another pair of plates (probe y), the impedance given by the two probes will be different, even if the plates are of the same size and separation. To measure the effect of frazil ice on the impedance of the ice-present sensor probe, as compared to the ice-free reference probe, an impedance bridge may be set up as shown in Fig. 1. For the bridge, the fractional
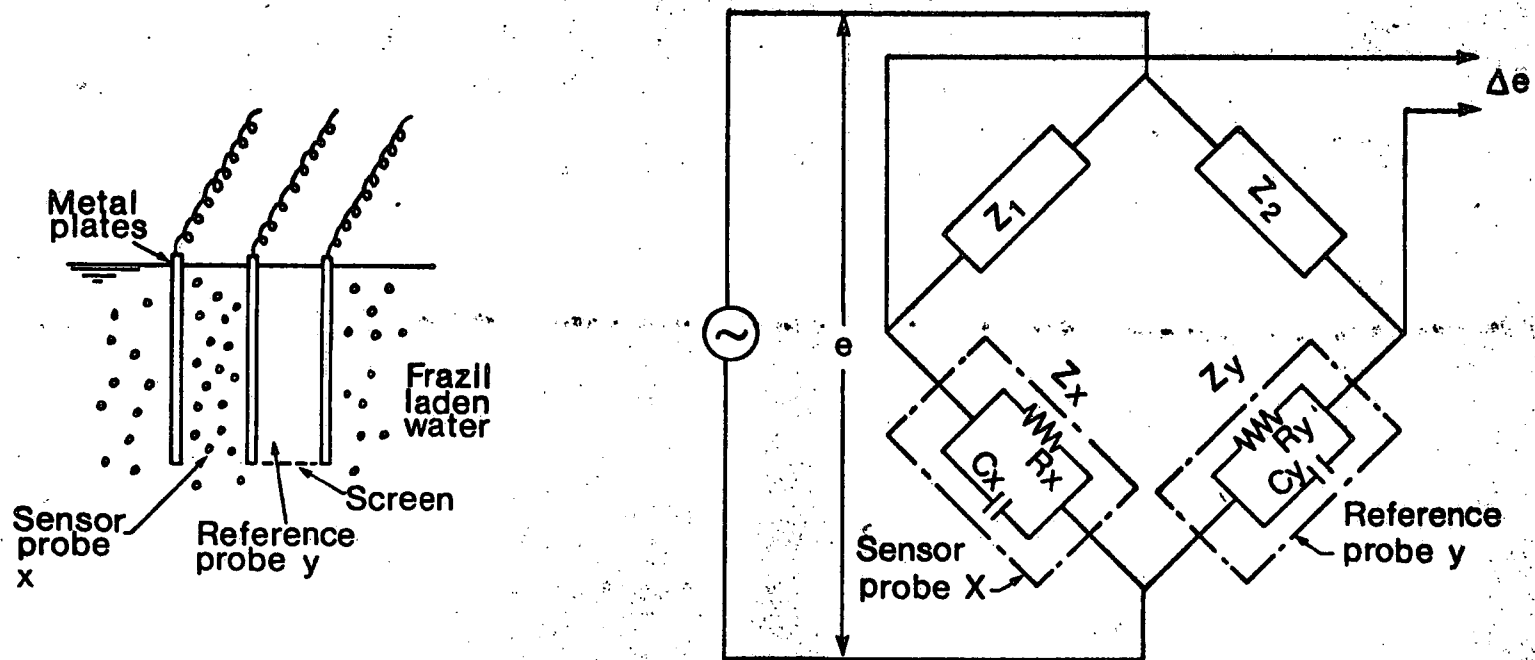
FIG.1 EQUIVALENT CIRCUIT OF 3 PLATES IMMERSED IN FRAZIL LADEN WATER AND
THE BRIDGE FOR MEASURING IMPEDANCE CHANGES.

voltage drop across the two measuring points is

$$\Delta = \frac{\Delta e}{e} = \frac{z_1}{z_1 + z_x} - \frac{z_2}{z_2 + z_y} \qquad \cdots\cdots\cdots (1)$$

where z is impedance and the subscripts indicate the four arms of the bridge.

Since z_y is not affected by the concentration of frazil ice c in the sensed volume of the sensor probe, and z_1 and z_2 can be made constant by design for a given frequency, the differentiation of Equation (1) with respect to c is given by

$$\frac{d\Delta}{dc} = \frac{d}{dc} \left(\frac{z_1}{z_1 + z_x} \right) \qquad \cdots\cdots\cdots\cdots (2)$$

Since z_x is a function of its resistance component, R_x, and reactance component, X_{cx}, and the latters are in turn functions of frazil ice concentration in the sensor probe, by chain differentiation rule, the above equation becomes*

$$\frac{d\Delta}{dc} = - \frac{z_1}{(z_1 + z_x)^2} \left(\frac{\partial z_x}{\partial R_x} \frac{dR_x}{dc} + \frac{\partial z_x}{\partial X_{cx}} \frac{dX_{cx}}{dc} \right) :$$

$$\cdots\cdots\cdots\cdots (3)$$

It is seen from Fig. 1 that z_x is given by

$$z_x = \frac{R_x X_{cx}}{R_x + X_{cx}} \qquad \cdots\cdots\cdots\cdots\cdots (4)$$

---

*For clarity of mathematical expression, the imaginary number indicator j associated with reactance is absorbed into X_{cx} and other similar reactance notations in this report.

The application of the above equation in Equation (3) gives

$$\frac{d\Delta}{dc} = \frac{-z_1}{(z_1 + z_x)^2} \left[\left(\frac{X_{cx}}{X_{cx} + R_x} - \frac{R_x X_{cx}}{(X_{cx} + R_x)^2} \right) \frac{dR_x}{dc} \right.$$

$$\left. + \left(\frac{R_x}{X_{cx} + R_x} - \frac{R_x X_{cx}}{(X_{cx} + R_x)^2} \right) \frac{dX_{cx}}{dc} \right] \quad \ldots \ldots (5)$$

To evaluate dR_x/dc and dX_{cx}/dc in the above equation, one needs to know the functional form of R_x and X_{cx}. The resistance between the two plates of the reference probe is*

$$R_y = \frac{\rho_0 S}{A} \quad \ldots \ldots \ldots \ldots \ldots \ldots \ldots \ldots (6)$$

where ρ_0 is the resistivity of the ice-free water and A and S are the plate surface area and the separation between the plates respectively. For the sensor probe, the presence of frazil ice reduces the conductive volume and hence increases the resistivity of the medium between the plates. If the frazil ice is assumed to be finely and uniformly suspended in the water, the increase in resistivity will be proportional to the volumetric presence of frazil ice in the water, and one may write

$$R_x = \frac{\rho_0}{(1-c)} \frac{S}{A} \quad \ldots \ldots \ldots \ldots \ldots \ldots \ldots (7)$$

---

*Strictly speaking, eq. (6) is only correct when the two plates are very close together and the stray effect is negligible. For plates of some distance apart, a corrective coefficient has to be introduced. This coefficient is not shown here because it will be cancelled out subsequently and will not affect the final theoretical outcome.

From Equations (6) and (7), one has

$$\frac{R_x}{R_y} = \frac{1}{(1-c)} \quad \dots \dots \dots \dots \dots \dots \dots \quad (8)$$

and its differentiation with respect to c gives

$$\frac{dR_x}{dc} = \frac{R_y}{(1-c)^2} \quad \dots \dots \dots \dots \dots \dots \quad (9)$$

The capacitance formed by the two plates of the reference probe
is given by *

$$C_y = \varepsilon_{H_2O} \frac{A}{S} \quad \dots \dots \dots \dots \dots \dots \quad (10)$$

where ε_{H_2O} is the absolute dielectric constant of water. For the sensor

probe, because of the presence of frazil ice, the dielectric constant ε_x

will be different from ε_{H_2O}. Intuitively speaking, ε_x should

be a function of ε_{H_2O}, the dielectric constant of ice ε_{ice}, the con-

centration of frazil ice in the sensor probe and some other secondary

factors. Since the exact functional relationship is not known, one may

assume a simple proportional law of

$$\varepsilon_x = (1 - c) \varepsilon_{H_2O} + c \varepsilon_{ice} \quad \dots \dots \dots \dots \quad (11)$$

The capacitance formed by the two plates of probe x, therefore, is given

by

$$C_x = \left[(1 - c) \varepsilon_{H_2O} + c \varepsilon_{ice} \right] \frac{A}{S} \quad \dots \dots \dots \quad (12)$$

_____

*See footnote preceeding page.

- 7 -

The reactances produced by C_x and C_y are, respectively

$$X_{cx} = - \frac{j}{2\pi f C_x} \quad \text{and} \quad X_{cy} = - \frac{j}{2\pi f C_y} \quad . . (13)$$

where $j = \sqrt{-1}$ and f is the frequency of the applied voltage. From Equations (10), (12) and (13), one obtains

$$\frac{X_{cx}}{X_{cy}} = \frac{C_y}{C_x} = \frac{1}{1 - c + c\gamma_\epsilon} \quad . . . . (14)$$

where

$$\gamma_\epsilon = \frac{\epsilon_{ice}}{\epsilon_{H_2O}} = \text{ratio of dielectric constants} \quad . . (15)$$

The differentiation of Equation (14) with respect to c gives

$$\frac{dX_{cx}}{dc} = \frac{1 - \gamma_\epsilon}{(1 - c + \gamma_\epsilon c)^2} X_{cy} \quad . . . . (16)$$

The substitution of Equations (9) and (16) into Equation (5) and then the expression of z_x, R_x and X_{cx} by Equations (4), (8), and (14), will produce a rather complicated function of $d\Delta/dc$ of the form of

$$\frac{d\Delta}{dc} = f\left(z_1, c, X_{cy}, R_y, \gamma_\epsilon\right) \quad . . . . (17)$$

and its integration will give the relationship between the signal output Δ and frazil ice concentration. Although the mathematical operations for obtaining the final relationship is numerically possible, it is not ad-

- 8 -

visable for an instrument to be based on such a complicated mathematical relationship. The relationship can be greatly simplified by imposing some constraints to the bridge circuit.

It is seen from Equation (4) that if X_{cx} is very much larger than R_x, z_x will be approximately equal to R_x. Conversely, if R_x is very much greater than X_{cx}, z_x will approach X_{cx}. For the former case, from

$$\left| \frac{-j}{2\pi f C_x} \right| \quad >> \quad R_x \quad \cdots \cdots (18)$$

and Equations (8) and (14), one has

$$\frac{1 - c + c\, \gamma_\varepsilon}{2\pi f C_y} \quad >> \quad \frac{R_y}{1 - c} \quad \cdots \cdots (19)$$

The substitution of Equations (6) and (10) into the above equation gives

$$f \quad << \quad \frac{1 - c + c\, \gamma_\varepsilon}{2\pi\, \varepsilon_{H_2O}\, \rho_0} \quad \cdots \cdots (20)$$

Since the largest value of γ_ε can only be about unity and under both laboratory and field conditions, frazil ice concentration seldom exceeds a few percent. The terms containing c in the above equation may be dropped without seriously affecting the equation. The resistivity of the ice-free water in the reference

probe ρ_0 is not a constant but decreases continuously as ice is formed and impurities are rejected into the water. If the conducting capability of water is considered to be proportional to the number of ions in the water, one may write

$$\rho_0 \;=\; (1 - \bar{c})\; \rho_{H_2O} \qquad \cdots \cdots \cdots \cdots \cdots (21)$$

where ρ_{H_2O} is the resistivity of the water at 0^0C but before the production of ice and $\bar{c}$ is the mean frazil ice concentration in the water. Since $\bar{c}$ is of the same order of magnitude as c, it may also be dropped from the above equation and approximately gives $\rho_0 \simeq \rho_{H_2O}$. With the above discussions, Equation (20) is reduced to

$$f \;\ll\; \frac{1}{2\pi \; \varepsilon_{H_2O}\; \rho_{H_2O}} \qquad \cdots \cdots \cdots \cdots \cdots (22)$$

The value of the absolute dielectric constant of water is approximately

$$\varepsilon_{H_2O} \;=\; 80\; \varepsilon_{vacuum}$$

$$\;=\; 80 \;\times\; \frac{1}{36\pi} \;\times\; 10^{-9} \quad \text{Farad/m}$$

and the typical value of ρ_{H_2O} of natural water is

$$\rho_{H_2O} \;=\; 20 \quad \text{ohm-m}$$

The substitution of the above values to Equation (22) gives

$$f \quad << \quad 10^7 \quad Hz \qquad \ldots \ldots \ldots \ldots \ldots \text{(23)}$$

When the above condition is satisfied, the reactance X_{cx} may be ignored and one has

$$z_x \quad = \quad R_x \qquad \ldots \ldots \ldots \ldots \ldots \ldots \text{(24)}$$

On the other hand, if

$$f \quad >> \quad 10^7 \quad Hz \qquad \ldots \ldots \ldots \ldots \text{(25)}$$

then the resistance R_x may be ignored from Equation (4) and one has

$$z_x \quad = \quad X_{cx} \qquad \ldots \ldots \ldots \ldots \ldots \text{(26)}$$

The frequency of 10^7 Hz is in the h-f (high frequency) range or the decametric wave range. There is no technical difficulty in the present technology in both furnishing Equations (23) and (25) and handling the signals. Thus, by choosing an appropriate frequency, the bridge can be made either resistance or reactance predominant.

When Equation (23) is satisfied, Equation (5) is reduced to

$$\frac{d\Delta}{dc} \quad = \quad \frac{-z_1}{(z_1 + R_x)^2} \quad \frac{dR_x}{dc} \qquad \ldots \ldots \ldots \ldots \text{(27)}$$

The substituting of Equations (8) and (9) into the above equation and the assignment of z_1 to consist of resistance R_1 alone give

$$\frac{d\Delta}{dc} \doteq \frac{-R_y/R_1}{(1 - c + R_y/R_1)^2} \qquad \ldots \ldots \ldots (28)$$

Since c is small compared to unity, it may be dropped from the right hand side of the above equation without seriously affecting the outcome. Thus, one has

$$\frac{d\Delta}{dc} = \frac{- R_y/R_1}{(1 + R_y/R_1)^2} \qquad \ldots \ldots \ldots (29)$$

The resistance between the two plates of probe y at 0^0C but before the production of ice in the water is given by

$$R_{y_0} = \rho_{H_2O} \frac{S}{A} \qquad \ldots \ldots \ldots \ldots \ldots (30)$$

From the above equation and Equations (6) and (21), one sees

$$R_y \doteq (1 - \overline{c}) R_{y_0} \qquad \ldots \ldots \ldots \ldots \ldots (31)$$

The substitution of the above equation in Equation (29) and the writing of

$$\frac{R_{y_0}}{R_1} = N \qquad \ldots \ldots \ldots \ldots \ldots \ldots (32)$$

- 12 -

give

$$\frac{d\Delta}{dc} = \frac{(\bar{c} - 1) N}{\left[1 + (1 - \bar{c}) N\right]^2} \qquad \ldots \ldots \ldots \ldots (33)$$

and the integration of the above equation gives

$$\Delta = \frac{(\bar{c} - 1) N}{(1 + N - \bar{c} N)^2} c \qquad \ldots \ldots \ldots \ldots (34)$$

which is a linear relationship. The above equation is integrated under the boundary condition that $\Delta = 0$, when $c = 0$. This boundary condition requires that the bridge should be balanced at zero ice presence in the sensor probe.

Strictly speaking, Equation (34) is not a linear relationship because the proportional coefficient is a function of $\bar{c}$ and which changes as frazil ice is continuously formed. Therefore, except for instantaneous measurement, such as for obtaining the concentration profile along a vertical at a given instance, the signal output and frazil ice concentration in probe x are not linearly proportional. However, since $\bar{c}$ is small compared to unity, the effect of $\bar{c}$ on the constancy of the proportional coefficient of Equation (34) should not be great.

Equation (34) shows that the signal output from the bridge depends on the resistance ratio N. Since the conductivity of natural water varies over a wide range from place to place, N will depend on the source of water for a constant R_1 on the bridge. From the above, one sees that the signal-frazil ice concentration relationship may not be calibrated from one sample of water for

other samples of water. For practical use of the instrument, the bridge should be so designed as to give a constant N for water of different conductivity. Electrically, this can be easily done, as will be discussed later in the report.

When high frequencies satisfying Equation (25) are used, Equation (5) is reduced to

$$\frac{d\Delta}{dc} = \frac{-z_1}{(z_1 + X_{cx})^2} \frac{dX_{cx}}{dc} \qquad \ldots \ldots \ldots (35)$$

The substitution of Equations (14) and (16) into the above equation and the assignment of z_1 to consists of reactance X_{c_1} alone gives

$$\frac{d\Delta}{dc} = \frac{-(1 - \gamma_\epsilon) X_{cy}/X_{c_1}}{(1 - c + \gamma_\epsilon c + X_{cy}/X_{c_1})^2} \qquad \ldots \ldots \ldots (36)$$

Denoting

$$M = \frac{X_{cy}}{X_{c_1}} = \frac{C_1}{C_y} \qquad \ldots \ldots \ldots \ldots \ldots \ldots (37)$$

where C_1 is the capacitance producing X_{c_1} and dropping the terms containing c on the right-hand side of Equation (36) because of their relatively small magnitude, results in

$$\frac{d\Delta}{dc} = \frac{(\gamma_\epsilon - 1) M}{(1 - M)^2} \qquad \ldots \ldots \ldots \ldots \ldots (38)$$

- 14 -

The integration of the previous equation gives

$$\Delta = \frac{(\gamma_\varepsilon - 1) M}{(1 - M)^2} c \qquad \ldots \ldots \ldots \ldots (39)$$

a linear relationship similar to Equation (34). The boundary condition leading to the above equation also requires that the bridge is balanced at zero frazil ice concentration in the sensor probe.

Comparing Equations (34) and (39), one sees that while the former is sensitive to $\bar{c}$, the latter is not affected by the production of ice. Also, while N in Equation (34) is affected by the conductivity of water for a given R_1, M in Equation (39) is not affected by the source of water. Thus, if the technical difficulty of employing a capacitance bridge and a resistance bridge is about the same and the costs are comparable, capacitance sensing of frazil ice is preferable in that Equation (39) is "truer" linear than Equation (34) and that one need not worry about the change of M, from one source of water to the other.

INSTRUMENT DEVELOPMENT

The development work reported herein aimed to verify the theoretical principles shown in the last section and is defined as phase I of the development. The further refinement of the theory and the production of a manufacturable prototype instrument will be left to phase II of the development. During phase I of the development, the first intention was to develop an experimental instrument based on the capacitance sensing principle. Such a plan had to be postponed because the company under contract for the design and construction of the hardware did not have a high frequency generator and some now appeared trivial technical problems. The plan was changed to the development of an experimental instrument based on the resistance sensing principle and its testing.

a. The Probe

Plate 1 is a photograph of the experimental probe. It consists of three stainless steel plates 1 cm wide x 2 cm long x 1 cm separation. Each plate was soldered onto two brass stems of 1 mm in diameter. The stems were 1.5 cm long with fine, insulated resistance wire wound on them as heaters. The coils on the two stems of each plate were connected in series but the heaters for the three plates were connected in parallel. Each heater coil had a resistance of approximately 8 ohms. The stems and heaters were together imbedded in scotch cast to prevent short circuits resulting from abrasion and burning out of the heaters' protective coatings. While the sides of the space between one pair of the plates (probe x) were open, the sides of the space between the second pair of plates (probe y) were sealed by tefron plates a little less than 1 mm thick. Small holes of 1 mm
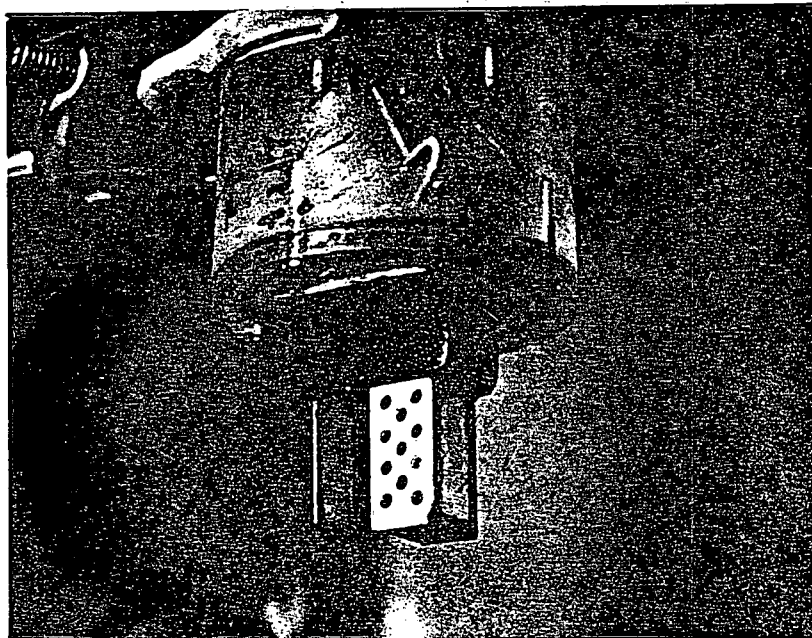
A. The Probe
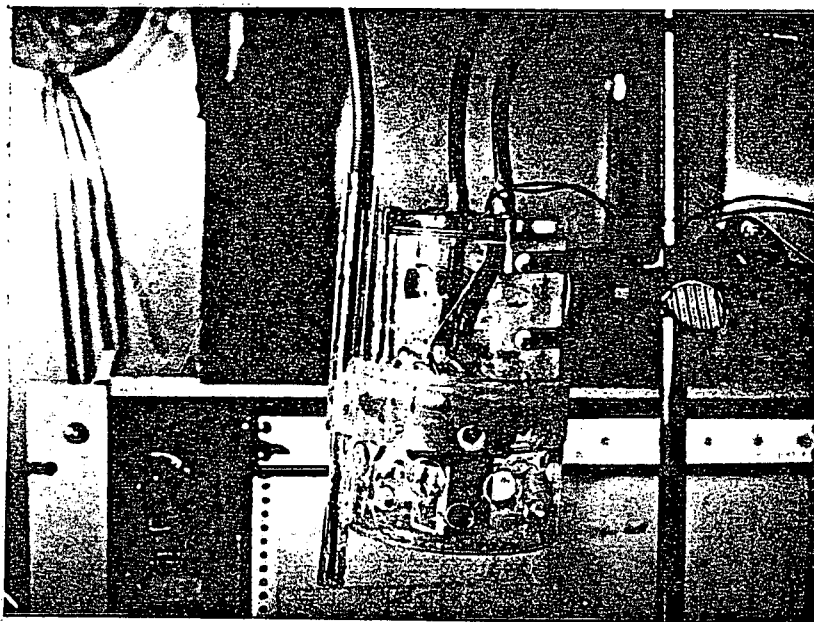
B. Probe with Protective Cap and Thermistor

PLATE 1. EXPERIMENTAL PROBE

in diameter were drilled on two side teflon plates for water to pass in and out of the probe to give a representative sample of the water to the reference probe. The bottom teflon plate was not perforated so the ice formed in the ambient water could not float into the sensed volume. Little ice could enter the reference probe from the side neither, because the perforated holes were perpendicular to the vertical direction of ice movement.

Ideally, the sensor probe and the reference probe should be identical and have the same resistance (and capacitance). However, this could not be done because, first of all, the probes were hand-made and secondly, while teflon plates were used as spacers between one pair of probe plates, they were absent between the second pair. The probes were also structurally not very rigid, accidental banging and twisting during their employment and cleansing could easily change the resistance and capacitance. A protective cap made of a short section of plexglass tubing with large holes drilled on the side and a nylon screen glued to the bottom was later used to protect the probes. The cylindrical body shown on Plate 1 above the probes was for housing the electrical joints and for providing a structural base for the probes. It was really too large for the above purposes and could be greatly reduced in size or eliminated altogether.

The heaters were for preventing the nucleation of ice on the probe plates, the adhesion of ice to the plates of the sensor probe and the formation of ice in the reference probe. If the rate of cooling of water is dT/dt, from supplying a heat flux by the heaters to compensate such a rate of cooling, one has

$$P = \frac{2 \times 4.186}{\eta} V \frac{dT}{dt} \qquad \cdots \cdots \cdots \cdots \cdots \quad (40)$$

for the reference probe, where P is the power to the reference probe's
heaters in watts, V is the volume of the reference probe in cm^3, dT/dt
is in ^{0}C/s, η is the efficiency of heat transmitted from the heaters to
the probes , 4.186 is a conversion factor and 2 is introduced because
only half of the heat is going to the sensed volume. The above eq-
uation tends to be conservative because, due to the slow motion of the
water in the caged reference probe, the rate of heat loss should be less
than that of the ambient water. From the above equation, the voltage of
the DC source applied to the reference probe's heaters, is given by

$$v = 2.89 \sqrt{\frac{RV}{\eta} \frac{dT}{dt}} \quad \text{volts} \qquad \cdots \cdots \cdots \cdots \quad (41)$$

where R is the resistance of the reference probe's heaters in ohms.
For the constructed experimental probe, because the heaters were
imbedded in insulation, a heating efficiency of η = 1.00 was assumed.
For the sensor probe (really the side plate that forms the sensor probe),
less heat is needed. Ideally, a feed-back system should be built into
the heaters, so that the plates of the sensor heater is maintained at a
temperature slightly above freezing. However, for the experimental probe,
because of easy construction, the heaters for the sensor probe were made the
same as the reference probe's heater and had the same heat input. It was
reasoned that since frazil ice is formed under turbulent conditions, the
heat dissipated into the water in the unconfined sensor probe is likely
to have diffused into the ambient water in a short time, instead of ac-
cumulating sufficiently around the probe to affect the reading. In

- 19 -

mathematical terms, one may say that since the convective variation of frazil ice concentration in the sensor probe very much outweighs the temporal variation which is affected by local heat input, the effect of local heat input to the total variation of frazil ice concentration may be overlooked.

The above reasoning is acceptable prior to ice formation, during the period of ice formation and when the concentration of frazil ice is low. When the concentration of frazil ice is high, the turbulence in the water is greatly suppressed and the movement of ice in the water is greatly reduced. Under such a situation, a high rate of heat input will lead to a fast melting of ice and an erroneous reading. If the frazil ice is assumed to stay in the sensor probe, then from the rate of heat flux and the consequent melting of ice, one obtains
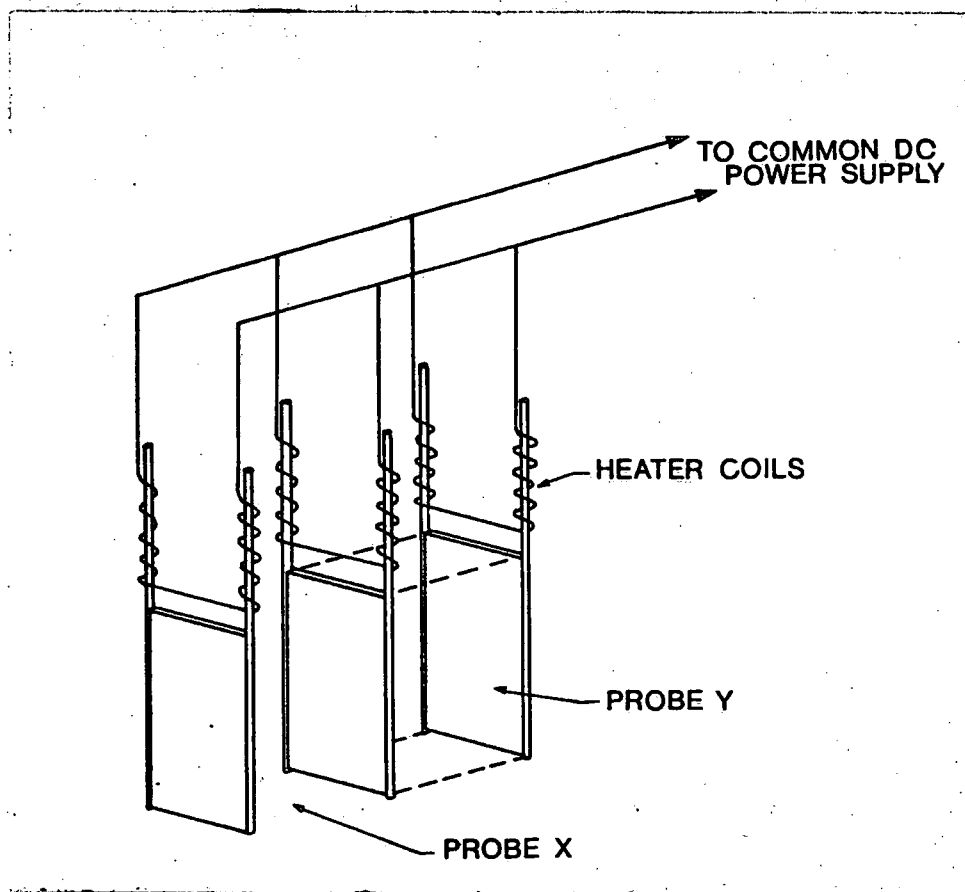
$$P = \frac{616 \, V \, c}{\eta} \left(\frac{dc/dt}{c} \right) \quad \text{watts} \quad \ldots \ldots (42)$$

where $(dc/dt)/c$ is the relative time rate of frazil ice concentration reduction in $\sec^{-1}$ and its reciprocal gives the time in second for all the ice to melt. For the experimental probe, Equation (40) was used to regulate the heaters prior to and during frazil ice formation and Equation (42) was used after frazil ice was formed in the experiments.
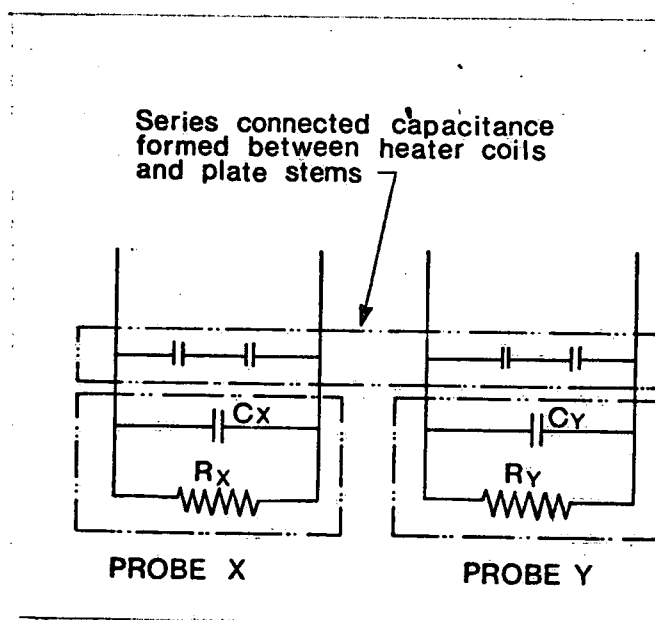
For good heat conduction from the heater to the probe plates, the heating coils have to be tightly wound against the plate stems and this introduces electronic implications because high capacitance is formed between the heating coils and the probe stem. If the heaters are connected to a common power source, as in the case of the experimental probe,

then, in addition to the capacitance formed between two probe plates, there are two capacitances formed by the coils and the stems and connected in series for each probe, as shown in Fig. 2. For the experimental probe, the additional high capacitance made the sensing bridge an impedance bridge instead of a resistance bridge. Before the heaters were imbedded into scotch cast, the seeping of water into the space between the coils and the stems had frequently upset the balance of the bridge. The presence of the additional capacitances had been overlooked and it took sometime before their discovery. Since the capacitance between the heating coils and the probe stems can be quite high in comparison to the capacitance between two probe plates, it can completely mask the latter and render an instrument built on the capacitance sensing principle in-operational. To minimize the effect of this unwanted large capacitance, for an instrument built on the resistance sensing principle, one may lower the frequency of the A. C. voltage applied to the bridge. For an instrument built on the capacitance sending principle, the corrective measures are more difficult and require further thinking. A simple way to eliminate this additional capacitance is to have independent power supplies to the heaters of each probe plate. However, this requires cumbersome power sources and is technically and engineeringly unsound.

Strictly speaking, the outer surface of the side plates of the probes should be insulated as to confine the sensed volume to within the probes. For the experimental probe, however, this was not done because the contractor could not find a suitable insulating material that would cling tightly to stainless steel. Since the construction of the experimental probe confined most of the electric line to the space between the plates, the stray effect caused by the exposed outer plate surfaces was overlooked.

TO COMMON DC
POWER SUPPLY

HEATER COILS

PROBE Y

PROBE X

Heater Arrangement of Experimental Probe

Series connected capacitance
formed between heater coils
and plate stems

C_X

R_X

C_Y

R_Y

PROBE X   PROBE Y

Equivalent Circuit of Probe with Heaters

FIG. 2. CAPACITANCE INTRODUCED BY HEATERS

b. The Circuitry

Based on the earlier theoretical investigations, the essential components of a basic instrument based on resistance sensing are shown in the block diagram in Fig. 3. In the block diagram, the signal of frazil ice concentration is picked up by the bridge. In the bridge, resistances R_{xp} and R_{yp} and capacitances C_{xp} and C_{yp} are connected in parallel to probe x and probe y. They are for fine resistance and capacitance adjustments of the probes, because the two probes cannot be made exactly identical. If the frequency of the applied voltage is sufficiently low, C_{xp} and C_{yp} may be neglected altogether. The low-frequencied voltage is provided by the low-frequency generator in Fig. 3. Apparently, the frequency cannot be too low, otherwise polarization will come into play. The bridge output is fed into an amplifier by way of a transformer. The amplified signal, after being rectified, is shown on the signal display.

The block diagram on Fig. 3 can be advanced to that as shown on Fig. 4. In Fig. 4, the amplitude of the low frequency A.C. generator is made variable by means of a potentiometer R_A. The fine adjustment of resistance equilibrium of the bridge is also obtained by the use of a potentiometer (variable resistance) and the fine adjustment of capacitance equilibrium is provided by the use of a fixed capacitance C_{xp} and a variable capacitance C_{yp}. The range of C_{yp} to be twice the magnitude of C_{xp} means that C_{yp} can be adjusted to less than or greater than C_{xp} as much as the magnitude of C_{xp}. Switch S_1 can be connected to one of the terminals a, b, c and d. Because the resistances R_a, R_b, R_c and R_d are progressively one less than the other in that
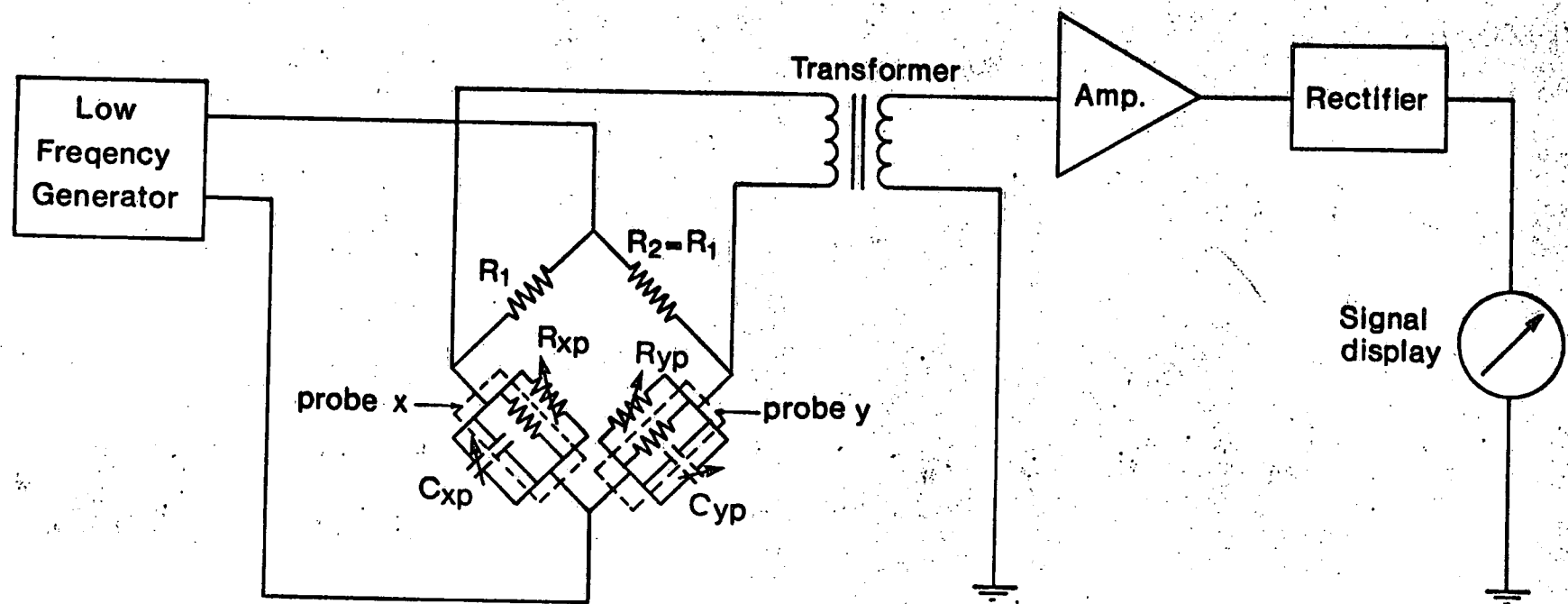
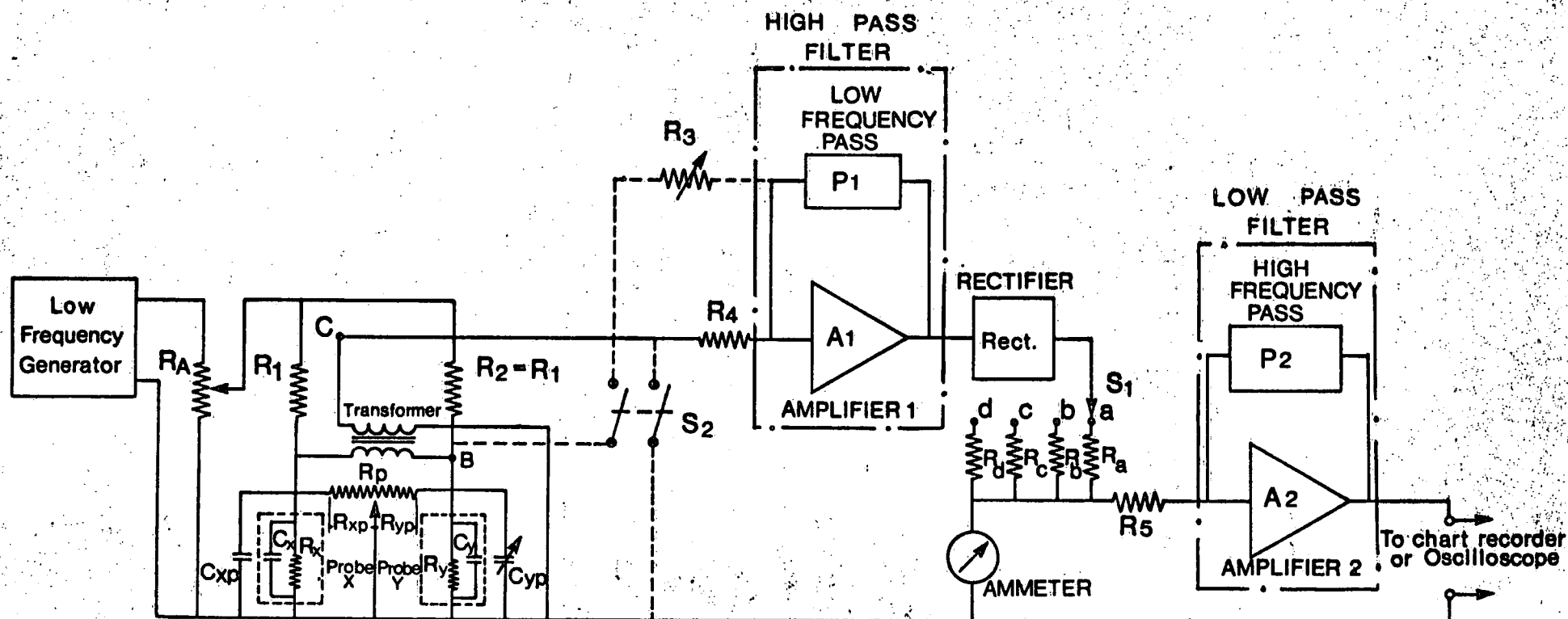Fig. 3 Block diagram for Frazil Instrument, based on resistance sensing.

Fig.4   Basic design of Frazil Ice Instrument.

order, for the same voltage output after the rectifier, the current through the resistances will be progressively larger.

The calibration of the signal display or the ammeter deflection can be made by connecting two known resistances R_x and R_y to the probe connectors with R_x, say 1% greater than R_y. The bridge will then become unbalanced and the unbalanced signal is shown by the ammeter. The deflection of the ammeter can be made to reach the meter's full range by adjusting the amplitude of the A.C. voltage input to the bridge through R_A. The replacement of R_x and R_y by the sensor and the reference probes then will enable the instrument to sense frazil ice concentration theoretically from 0 to 1%.

If the above calibration is done for switch S_1 at position d, say, and the ratio of the resistances is $R_a : R_b : R_c : R_d = 10 : 5 : 2 : 1$, a full range deflection of the ammeter when S_1 is at d, will only give ammeter deflections of 0.5, 0.2 and 0.1 of the full range, respectively, when switch S_1 is switched to positions c, b and a. In other words, four different sensitivity ranges of 0-1%, 0-2%, 0-5% and 0-10% can be obtained by simple switching of S_1 to the four different positions. Although four sensitivity ranges, as shown above were used for the experimental instrument, there is no restriction for the number and sensitivity of the ranges. The above discussion is only quantitatively valid when the internal resistance of the signal output system is small compared with resistances R_a to R_d.

In describing the calibration procedure above, it was only required that R_x is 1% greater than R_y and the absolute value of R_y is not specified. It is seen from the earlier theoretical investigations (see Equation (29)) that the full deflection of the ampmeter is also affected by the absolute value of R_y. Thus, for different R_y's, R_A has to be adjusted each time. Because the conductivity of water from

different sources is different, this means R_y will change from one water sample to the other, or that the instrument has to be calibrated each time using an electrical resistor having exactly the same resistance as that between the two probe plates when immersed in the particular water. To overcome this problem, a calibration switch S_2 and a variable resistance R_3 shown by dashed lines in the block diagram on Fig. 4 were used in the experimental instrument. When S_2 is open, the calibration described earlier is not affected by the presence of R_3 and a full range deflection of the ammeter can be obtained by adjusting R_A as if R_3 were not there. After the full range deflection is obtained, the voltage at point C and the voltage at point B will have a one-to-one correspondence relationship. When S_2 is closed, the input to amplifier 1 will be the voltage at B, by way of R_3 instead of the voltage at C, by way of the constant resistor R_4. R_3 may now be adjusted to give a full range deflection of the ampmeter. After fixing this R_3 setting, any R_A setting that gives a full deflect of the ampmeter, by way of C will also give a full deflect of the ampmeter by way of B. With the above conclusion, for different values of R_y, because of different sources of water, one may close switch S_2 and adjust R_A for a full ampmeter deflection. Once this is obtained, the opening of S_2 and the placement of R_y and $R_x = 1.01R_y$ will also give a full meter deflection.

The above arrangement is only valid if the functional relationship between the potential at C and the potential at B is independent of the value of R_y, or rather, the ratio of R_2/R_y. This, however, is not the case because the earlier theoretical investigations show that the potential at C, which is really the bridge signal output, is a function of both R_x/R_y and R_2/R_y. On the other hand,

point B is on the arm of the bridge containing R_2 and R_y, the potential

at point B, therefore, should also be affected by R_2/R_y. Thus, the

functional relationship between the potential at C and the potential at

B depends on R_2/R_y and the calibration is physically unsound. The

above physical drawback was not perceived when designing the instru-

ment. R_3 and S_2 were not eliminated from the experimental instrument

after the above drawback was found because for the evaluation tests,

water from the same tap was used. The small daily variation of the

resistivity of the water probably would only have a negligible effect

on the initial calibration and the incorporation of R_3 and S_2 in the

instrument would make the daily operation much easier. For the final

version of the instrument, the above part of the circuitry has to be

eliminated and replaced by a more appropriate circuit to be shown later

in the report.

For showing the signals on an oscilloscope and for recording

the signals on a chart or tape recorder, the signal input to the ammeter

is further amplified by Amplifier 2, as shown on the block diagram on

Fig. 4.

The detailed design of the experimental instrument is shown by

the circuit diagram on Fig. 5. It is seen from the circuit diagram that

a 50 kHz A.C. generator was used for the bridge. This frequency is suf-

ficiently low compared to the critical frequency of 10^7 Hz. The power

supply to the heater is not shown on the diagram. The ratios of R_a : R_b :

R_c : R_d : are not exactly 10: 5: 2: 1. Plate 2 is a photograph showing

the experimental instrument and its connection to the experimental probe.
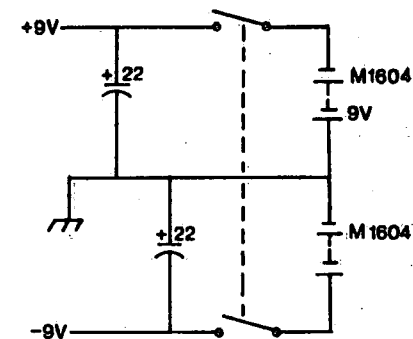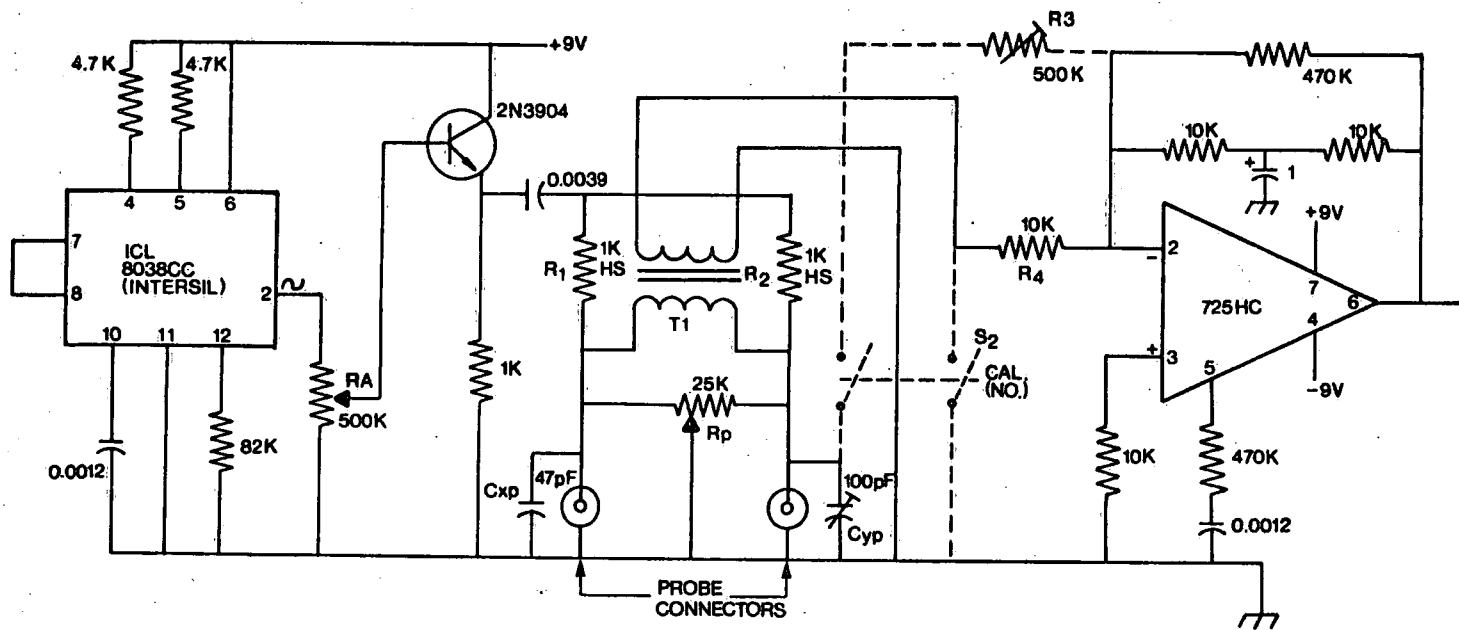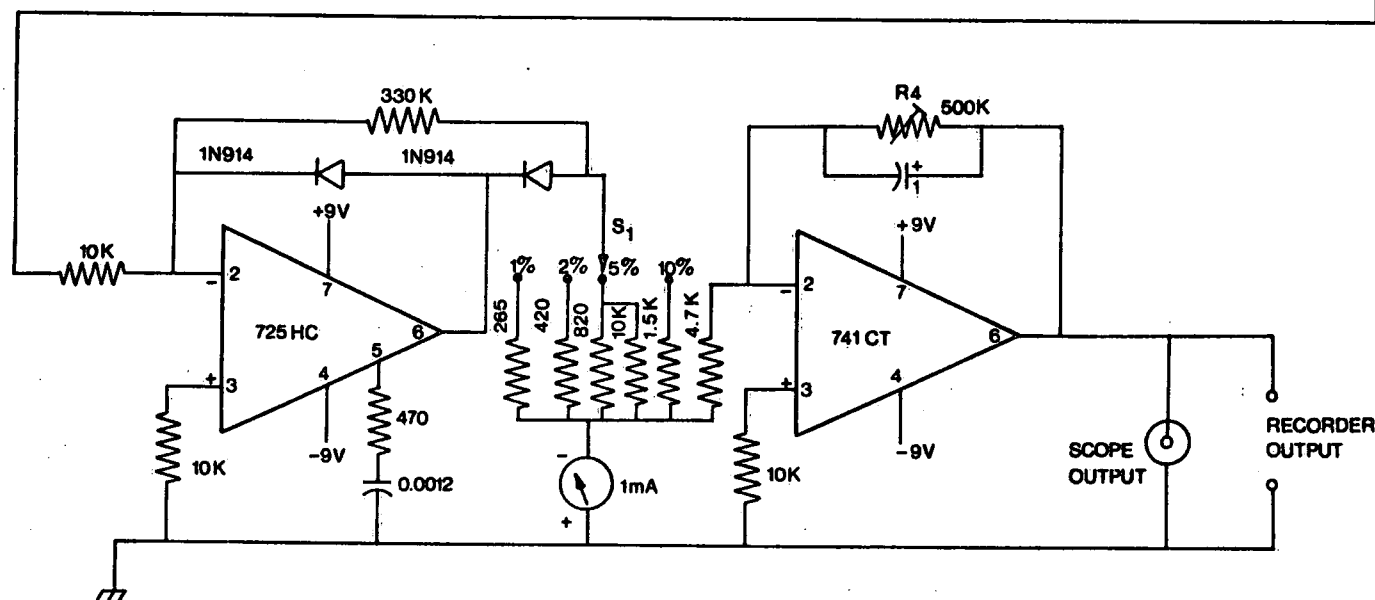
Figure 5   ELECTRONIC CIRCUIT OF EXPERIMENTAL INSTRUMENT FOR FRAZIL ICE SENSING
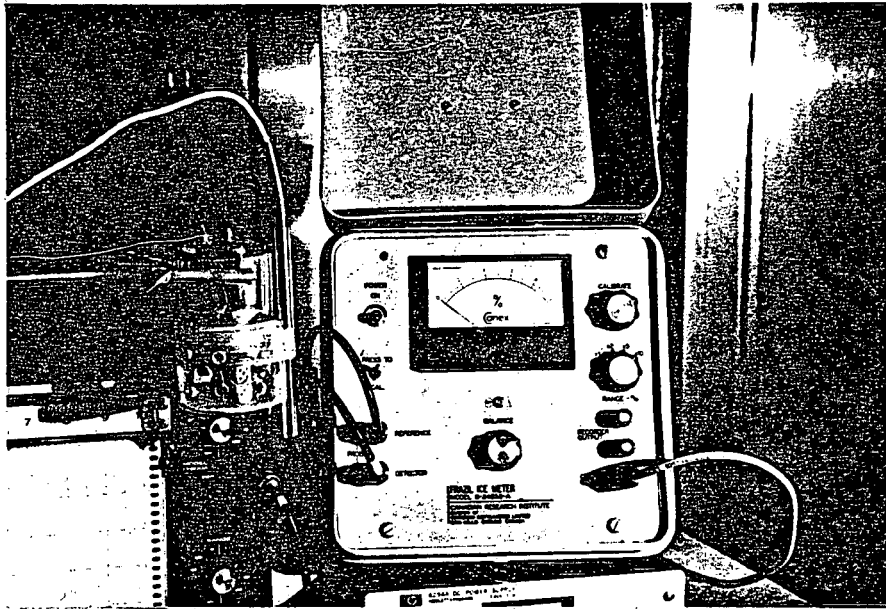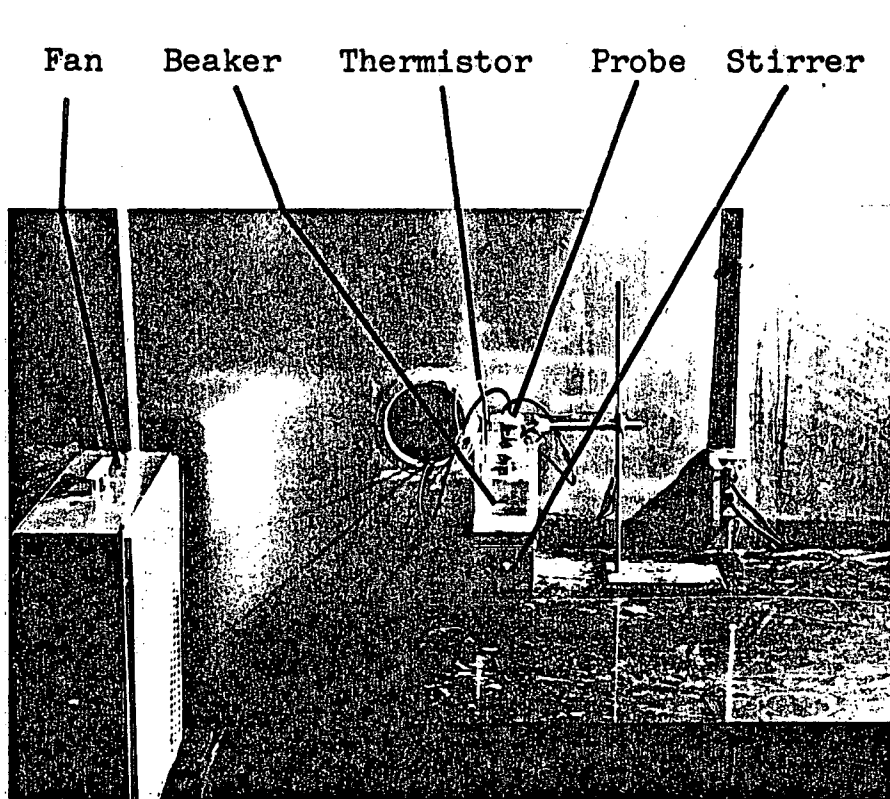
PLATE 2.   EXPERIMENTAL INSTRUMENT AND ITS
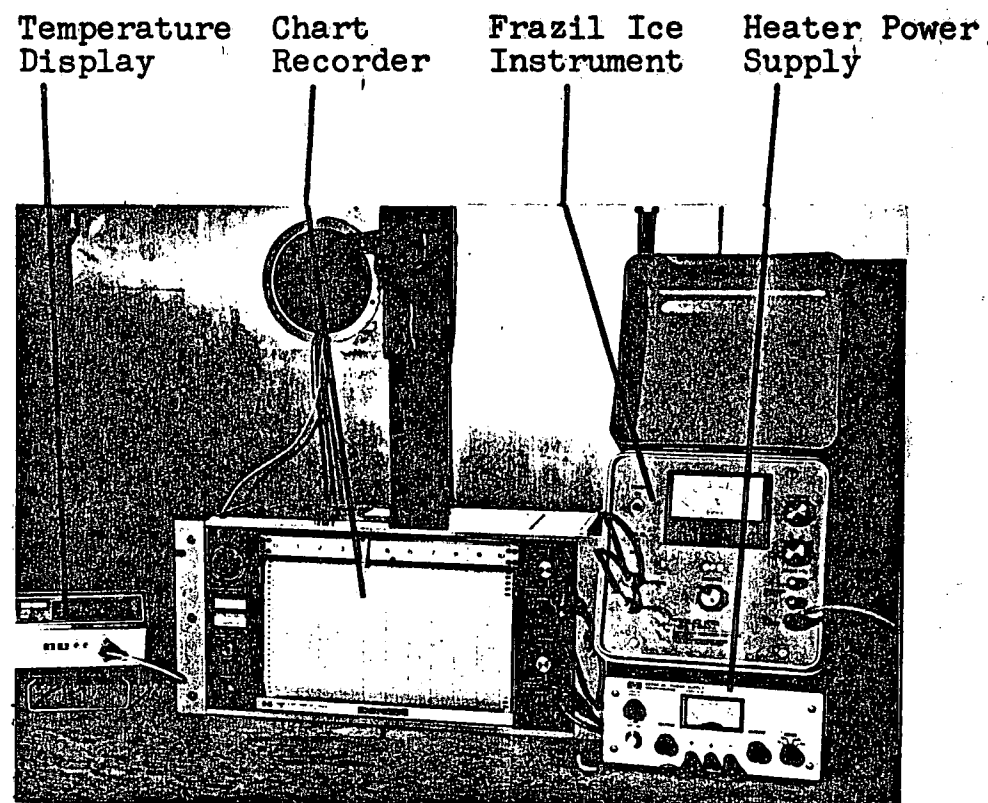CONNECTION TO THE PROBE

TESTING AND EVALUATION OF THE EXPERIMENTAL INSTRUMENT

The experimental instrument was tested in a cold room. The experimental set up is shown on Plate 3. It is seen from Plate 3 that the experimental probe was immersed in a 1000 ml beaker atop a magnetic stirrer. The turbulence in the beaker was generated by the swirl of a magnetic bar. The probe was so placed that the scotch cast base was just in the water. The protective cap was placed over the probe. The placement was carefully adjusted so that the screen at the end of the cap was very close to the end of the probe plates. The frazil ice in the probe therefore, was generated in the water inside the cap over the probe's depth. The stirrer was placed in front of a two-speed fan. By adjusting the stirrer and fan speeds, and the distance between the beaker and the fan, different cooling rates could be obtained. The fan and the stirrer greatly affected the cooling rate of the water, especially the former. When both the fan and the stirrer were off, the cooling rate was reduced by one or two orders of magnitude. A thermistor-type thermometer calibrated and accurate to 0.01^0C was secured to the protective cap. The temperature output was recorded by a chart recorder as well as displayed on a digital voltmeter outside of the cold room. The signal output from the probe was also chart-recorded. A D-C power supply provided the power to the heaters of the probe. For all the experiments, the cold room was maintained at about -10^0C.

The generation of turbulence by a magnetic stirrer has the advantage of eliminating spraying and splashing. The spontaneous seeding of frazil ice due to the falling of ice particles formed in the air as a consequency of spraying and splashing of the water is thus avoided.

Fan   Beaker   Thermistor   Probe   Stirrer

Temperature   Chart   Frazil Ice   Heater Power
Display   Recorder   Instrument   Supply

Inside the Cold Room   Outside the Cold Room

PLATE 3. EXPERIMENTAL SETUP FOR TESTING THE FRAZIL ICE INSTRUMENT

The experiments showed that when only the thermometer was placed in the beaker, there was little breaking of the water surface caused by the presence of the thermometer and the water could be quite easily supercooled to as much as -6^0C. However, when the experimental probe was placed in the beaker, there was some occasional breaking of the surface and that led to earlier spontaneous formation of frazil ice or surface ice. Generally speaking, with the presence of the probe, it was difficult to obtain more than -1^0C supercooling. The formation of ice in the experiments was initiated by seeding the supercooled water with a lump of ice. Ice was seen forming quickly as the seeding ice lump reached the magnetic bar and was broken up. Just before seeding, the fan was turned off and as soon as ice began to form, the magnetic stirrer was also turned off. Immediately after ice formation, the power input to the heaters of the probe was changed from that governed by Equation (40) to that governed by Equation (42).

The ice formed in the supercooled water was either of needle form or of flakal form. Plate 4 contains photographs showing these two forms of dynamic ice. A ruler is shown on the upper picture to give the size of the beaker and the ice crystals. The division of these two forms of ice was approximately -1.9^0C. For supercoolings above this critical temperature, needle frazil ice was formed and for supercoolings colder than this critical temperature, the flakal work was produced. While the needle frazil ice floated and moved slowly with the water, the flakal ice formed a bee-hive like, but much more irregular and complicated flakal work that effectively stopped the movement of the water. In the experiments that were testing the instrument, only needle frazil ice was formed.
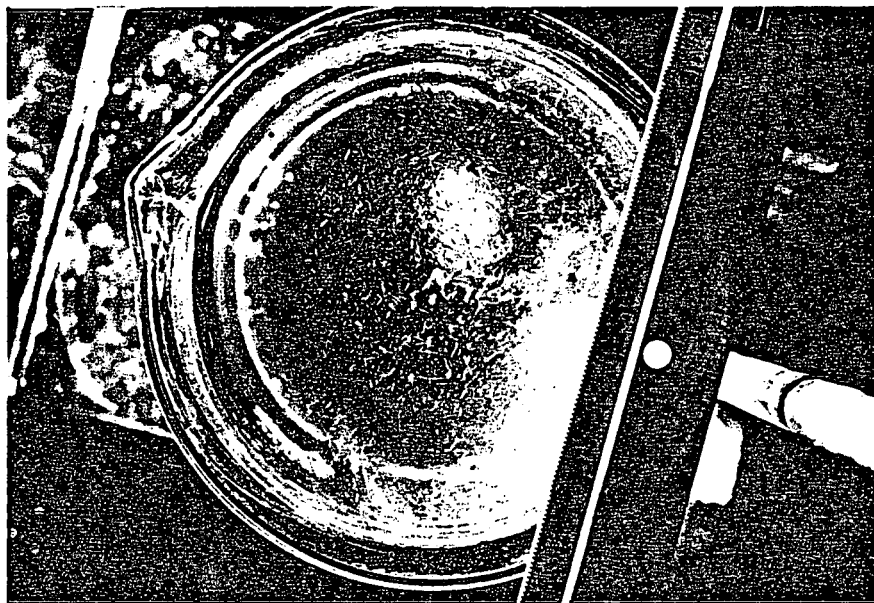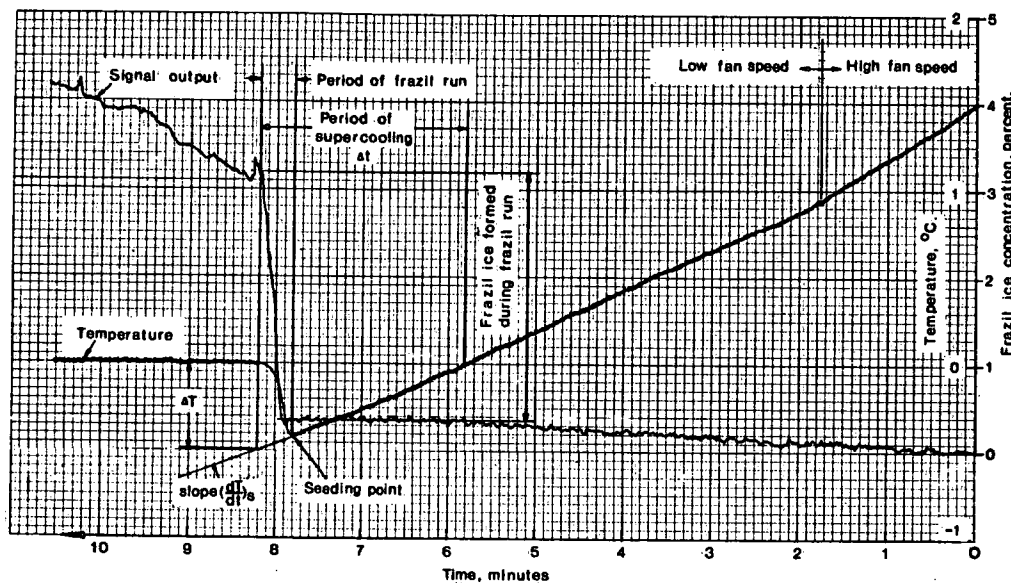
A. Needle Frazil Ice: Formed above $-1.9\ ^{\circ}C$

B. Flakal Ice Crystals: Formed below $-1.9\ ^{\circ}C$

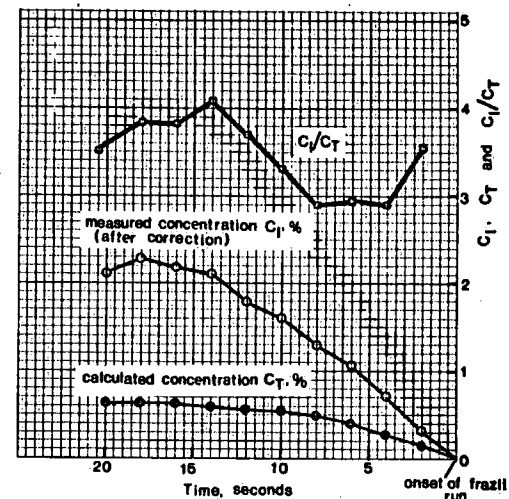PLATE 4. TWO TYPES OF DYNAMIC ICE FORMED IN THE EXPERIMENTS

Fig. 6a is the typical experimental output of a test and shows the simultaneous temperature and the instrument output recordings. It is seen from Fig. 6a that the temperature of the water decreased almost linearly under the tested conditions. The change of the cooling rate as the fan was switched from high to low can also be seen. The linear temperature depression continued to the minimum point at which frazil ice was seeded. As soon as ice was formed and the latent heat of fusion was released, it is seen from the temperature curve that the temperature of the water quickly rose to 0^0C and maintained that temperature as ice was continuously formed.

A clear correlation between the instrument's output and the temperature recording is seen from the diagram. Fig. 6a shows that the signal output increased rapidly following seeding, indicating an increasing frazil concentration in the water. The signal output increased much slower after the frazil run was finished and the water temperature reached 0^0C because the rate of heat loss was reduced by switching off the fan and the stirers. Following the frazil run, the ice formed was mainly surface ice. The slow upward drifting of the instrument signal prior to frazil formation was caused by the temperature dependence of the conductivity of water. Should probe x and probe y be exactly the same, the temperature effect on the conductance of these two probes would have compensated each other and there would have been no upward drifting. It is interesting to note from the diagram that after 0^0C was reached, the upward drifting of the signal was gone, indicating an independence of the conductivity of supercooled water on temperature.

Theoretically, the temperature and the signal output curve should rise at the same time because the formation of frazil ice is

a. Temperature depression and instrument signal output.

Signal output

Period of frazil run

Period of supercooling
Δt

Low fan speed ⟶ High fan speed

Frazil ice formed during frazil run

Temperature

ΔT

slope $\left(\frac{dT}{dt}\right)_s$ Seeding point

Time, minutes

Temperature, °C

Frazil ice concentration, percent.

c. Comparison of measured and calculated concentrations during the frazil run

C_I/C_T

measured concentration C_I, %
(after correction)

calculated concentration C_T, %

Time, seconds

onset of frazil run

C_I, C_T and C_I/C_T
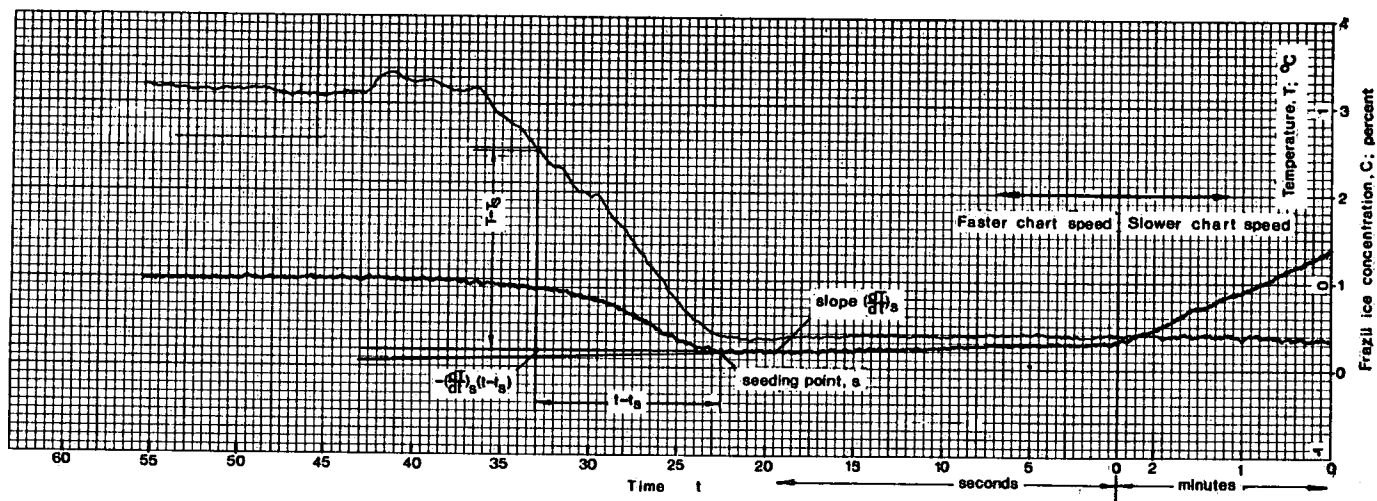
b. Expanded temperature and frazil ice recordings for the frazil run period.

$t-t_s$

Faster chart speed | Slower chart speed

slope $\left(\frac{dT}{dt}\right)_s$

$-\left(\frac{dT}{dt}\right)_s(t-t_s)$

$t-t_s$

seeding point, s

Time   t

seconds ⟶ | ⟵ minutes

Temperature, T; °C

Frazil ice concentration, C; percent

FIGURE 6.   Experimental result of an experiment.

accompanied by the liberation of latent heat and consequently the heating up of the water. Fig. 6a shows, however, that the temperature curve began to climb several seconds before the climbing up of the output signal. One should not be troubled by the above because it was caused by the mechanical inertia of the recorder, rather than by the incapability of the instrument. Fig. 6b is a simultaneous recording of Fig. 6a on another chart recorder at a faster speed. It is seen from Fig. 6b that the signal output curve in this case climbed slightly (about 1 second) ahead of the temperature curve.

The concentration of frazil ice as shown on Fig. 6 has to be corrected to give the true experimental frazil ice concentration because the experimental condition was different from the electrical calibration condition of the instrument. Before the experiments, the instrument was electrically calibrated with a resistance of 1000 Ω substituted for Ry and a resistance of 1100 Ω substituted for R_x and switch S_1 was connected to Ra for the 0 - 10% sensitive range. R_3 was also set under the above electrical calibration condition. It is seen from Fig. 4 that under such a calibration condition, when S_2 is closed, the voltage input to the amplifying circuit e_B, or the voltage at point B, is equal to half the excitation voltage to the sensing bridge.

For the experiments, the water used did not give a resistance of $Ry_0 \simeq Ry$ of 1 kΩ to the reference probe. Measurements of Ry_0 at the University of Waterloo (80 km from CCIW, an A. C. impedance bridge was not available at CCIW) gave values of Ry_0 from 350 to 425 Ω. If the mean resistance of $Ry_0 = 390$ Ω is assumed for the tested water, then to give a full ampmeter deflection when S_2 is closed, R_A in Fig. 4 has to be so

adjusted that the excitation voltage to the bridge will be

$$\frac{1000 + 390}{390} \; e_B = 3.56 \; e_B$$

which is 1.78 times the excitation voltage under the electrical calibration condition. Since the bridge output under the tested condition was Δ times the excitation voltage, the frazil ice concentration reading from the instrument under the tested conditions therefore should be divided by the factor of 1.78 to give the true Δ sensed by the bridge.

Due to calibration errors, it was noted later that the instrument was electrically calibrated not to give 100% full ampmeter deflection, but 90% ampmeter deflection instead. Because of these errors, the correction factor was modified from 1.78 to 1.62.

The lower resistance of the probes under the tested conditions than under electrical calibration affected not only the excitation voltage to the bridge, but the output of the bridge Δ also. Earlier theoretical investigations show that the signal output of the sensing bridge and the concentration of frazil ice in the sensor probe is related by Equation (34). The dropping of the terms containing $\bar{c}$, because of its small magnitude compared to unity, reduces Equation (34) to

$$\Delta = - \frac{N}{(1 + N)^2} c \quad \cdots \cdots \cdots \cdots \cdots \quad (43)$$

Under the electrical calibration conditions, one has $N = 1$, and the above equation is reduced to

$$\Delta = - \frac{c}{4} \quad \cdots \cdots \cdots \cdots \cdots \cdots \quad (44)$$

Under the experimental conditions, one has N = 0.39 and Equation (43) becomes

$$\Delta \simeq - \frac{c}{5} \quad . \quad . \quad . \quad . \quad . \quad . \quad . \quad . \quad . \quad . \quad . \quad . \quad . \quad . \quad . \quad . \quad . \quad (45)$$

Comparison of Equations (44) and (45) shows that, for the same ice concentration or the same change in resistance in the sensor probe as compared to the reference probe, the signal output from the bridge under the tested conditions would be 20% less than that under the electrical calibration conditions. Thus, the concentration of frazil ice as read from the instrument should be increased by 20% to give the "true" concentration. Taking the above into consideration, the earlier correction factor of 1.62 is further modified to 1.35.

From recordings similar to Fig. 6, the concentration of frazil ice at the end of the frazil ice runs were read off and corrected, and are shown on Table 1.

The concentration of frazil ice may also be calculated from the temperature depression curves. It is seen from Fig. 6 that theoretically the concentration of frazil ice at the end of the frazil run is given by

$$c = \frac{c_h \int_{\Delta t} - \frac{dT}{dt} \, dt}{h_L} \quad \times \quad 100\% \quad . \quad . \quad . \quad . \quad . \quad . \quad . \quad (46)$$

where c_h is the specific heat of water and is equal to 1 cal/g ^{0}C, dT/dt is the rate of temperature depression of the supercooling water, h_L is the latent heat of fusion and is equal to 80 cal/g and Δt is the time period from the onset of supercooling to the end of frazil run, which is given by the point of the temperature returning to 0^0C. It is seen from Fig. 6a

TABLE 1. **Frazil Ice Concentration measured by the instrument and calculated from the temperature depression curve.**

Test	ΔT °C	c_{int}%	c_t%	c_i%	c_i/c_t	mean c_i/c_t
1	0.39	1.86	0.4875	1.378	2.826	
2	0.44	2.28	0.55	1.689	3.071	
3	0.45	2.50	0.55625	1.852	3.329	3.259
4	0.46	2.92	0.575	2.163	3.762	
5	0.50	2.79	0.625	2.067	3.307	
6	0.51	3.76	0.6375	2.785	4.369	
7	0.51	2.05	0.6375	1.519	2.382	3.060
8	0.60	2.46	0.75	1.822	2.430	
9	0.62	2.20	0.775	1.630	2.103	
10	0.63	3.31	0.7875	2.452	3.113	
11	0.64	5.80	0.80	4.296	5.370	
12	0.65	2.80	0.8125	2.074	2.553	3.235
13	0.65	4.32	0.8125	3.200	3.938	
14	0.66	3.75	0,825	2.778	3.367	
15	0.68	3.40	0.85	2.519	2.963	
16	0.70	2.92	0.875	2.163	2.472	
17	0.74	3.88	0.925	2.874	3.107	
18	0.75	5.20	0.9375	3.852	4.109	
19	0.75	3.95	0.9375	2.926	3.121	3.520
20	0.80	5.05	1.0000	3.741	3.741	
21	0.82	3.85	1.025	2.852	2.782	
22	0.82	3.33	1.025	2.467	2.407	3.009
23	0.84	5.94	1.05	4.400	4.190	
24	0.87	3.90	1.0875	2.889	2.656	
25	0.97	8.40	1.2125	6.222	5.132	
26	1.02	5.52	1.275	4.089	3.207	
27	1.03	8.30	1.2875	6.148	4.775	4.480
28	1.07	8.72	1.3375	6.459	4.829	
29	1.09	8.20	1.3625	6.074	4.458	
					Median =3.31	mean =3.444

Note: ΔT = temperature depression, see Fig. 6a.

c_{int} = concentration of frazil ice as read from the instrument.

c_t = concentration of frazil ice calculated from the temperature depression curve.

c_i = instrument-read concentration of frazil ice after correction.

- 40 -

that approximately one has

$$c = \frac{-c_h \, \Delta T}{h_L} \times 100\% \qquad \dots \qquad (47)$$

where ΔT is obtained by projecting the temperature curve to the point

of regaining 0^0C. According to the above equation, the theoretical frazil

ice concentration was calculated for all the tests and listed on Table 1.

On Table 1, the ratio of the concentration of frazil ice as detected by the

instrument c_i, to the theoretical concentration of frazil ice c_t, is also

shown. The mean value of c_i/c_t is 3.44 and the median value is 3.31.

The linear correlation that passes through the origin as the physics

requires, and gives a 90% confidence, is approximately

$$c_i/c_t = \left(1 \pm \begin{array}{c} 0.52 \\ 0.28 \end{array} \right) 3.31 \qquad \dots \qquad (48)$$

The above correlation was for the end of the frazil runs.

Similar correlations may also be obtained for any instant within the

period of frazil runs. It is seen from the temperature depression

curve on Fig. 6a that before the seeding of frazil ice, the water has

been losing heat at a rate of c_h $(dT/dt)_s$, where $(dT/dt)_s$ is the negative

slope of the temperature curve before seeding. This ambient heat loss of

the supercooling water should remain approximately the same during the

short period of frazil formation. It is seen from Fig. 6a that during the

period of frazil run, because the liberation of latent heat accompanying the

formation of frazil ice, the temperature of the water climbed up instead of

continuing to fall. From the conservation of heat for any given instant,

one may thus write the following equation

$$c_h \frac{dT}{dt} = h_L \frac{dc}{dt} + c_h \left(\frac{dT}{dt}\right)_s \qquad \ldots \ldots \ldots \ldots (49)$$

The integration of the above equation gives

$$c = \frac{c_h}{h_L} \left[\left(T - T_s\right) - \left(\frac{dT}{dt}\right)_s (t - t_s) \right] \qquad \ldots \ldots (50)$$

where the subscript s indicates the instant of seeding at which the concentration of frazil ice is zero. The terms within the bracket in the above equation are readily measurable from the temperature depression curve as shown on Fig. 6b. Based on Equation (50), the concentration of frazil ice for the period of frazil run on Fig. 6b was calculated and is shown on Fig. 6c. On Fig. 6c, the concentration of frazil ice sensed by the instrument after correction, is also shown. The ratio of c_i/c_t for the period of frazil run, as seen from Fig. 6c, varied between 2.90 and 4.08 with a mean value of 3.46, which is not very much different from the value of 3.307 for the end of the test run, as shown on Table 1 (Test 5). Because of the mechanical inertia of the chart recorder, the seeding point shown on the temperature depression curve and the frazil ice concentration curve on Fig. 6b (and other similar recordings) are slightly different. It was rather subjective to re-align these two points together during constructing Fig. 6c. The above alone, could easily give 5 to 10% difference in the value of c_i/c_t.

From the laboratory tests, one may conclude that the experimental instrument can sensitively and quantitatively detect the presence of frazil ice. An instrument based on the theoretical principles shown in the report, therefore, will have great promises.

DISCUSSIONS ON THE EXPERIMENTAL INSTRUMENT AND ITS EVALUATION

Although for individual tests the experimental instrument gave good quantitative measurements of frazil ice, the correlation between the instrument output and the calculated frazil ice concentration appeared to vary from test to test. For the performed tests, Equation (48) shows that the c_i/c_t ratio could be 52 percent above and 28 percent below the median value at 90 percent confidence. Apparently such a highly varied correlation is not satisfactory for an instrument intended for scientific measurements.

A reason for the above variation in the correlation relationship is the not all perfect calibration technique. Although in the tests only the frazil ice formed inside the protective cap was sensed, in this small confined volume, the distribution of frazil ice was still not uniform. It is seen from Plate 4 that the frazil ice crystals tended to cluster together to give a spatial variation of their concentration. Whether the sensor probe was in the "thick" or "thin" regions could produce a substantial difference in signal output.

The above reason, however, is minor compared to the weak design of the bridge; spatial variation in concentration in the small confined volume alone, should not give two measurements that are 2.5 times different under almost identically tested conditions (see Table 1, tests 9 and 11). The weak design of the bridge is caused by the parallel connection of the adjustment resistance R_{xp} and R_{yp}. It is seen from Fig. 4 and 5 that the equivalent resistance on the x and y arms of the bridge are respectively,

$$R_{ex} = \frac{R_x R_{xp}}{R_x + R_{xp}} \quad \text{and} \quad R_{ey} = \frac{R_y R_{yp}}{R_y + R_{yp}}$$

$$\ldots \ldots \ldots \ldots \ldots (51)$$

When the bridge is balanced, one has $R_{ex} = R_{ey}$, or

$$\frac{R_x R_{xp}}{R_x + R_{xp}} = \frac{R_y R_{yp}}{R_y + R_{yp}} \qquad \dots \dots \dots \dots (52)$$

From Fig. 4, one also sees that

$$R_{yp} = R_p - R_{xp} \qquad \dots \dots \dots \dots \dots (53)$$

The substitution of the above equation into Equation (52) and its expansion lead to

$$\left(1 - \frac{R_y}{R_x}\right)\left(\frac{R_{xp}}{R_p}\right)^2 + \left(\frac{R_y}{R_x} - 2\frac{R_y}{R_p} - 1\right)\frac{R_{xp}}{R_p} + \frac{R_y}{R_p} = 0$$

$$\dots \dots \dots \dots \dots (54)$$

Since in the instrument design R_p is much greater than R_y, one has

$$\frac{R_y}{R_p} \to 0 \qquad \dots \dots \dots \dots \dots \dots (55)$$

The application of the above condition to Equation (54) leads to

$$\frac{R_{xp}}{R_p} \to 1 \qquad \text{or} \qquad R_{xp} \to R_p \qquad \dots \dots \dots \dots (56)$$

Since the bridge is symmetric, one also has

$$R_{yp} \to R_p \qquad \dots \dots \dots \dots \dots \dots (57)$$

The simultaneous existence of Equations (56) and (57) means that the balance of the bridge is not sensitive to the potentiometer R_p. A small variation in R_x relative to R_y can cause a wide change in R_{yp} (or R_{xp}) for the bridge to regain balance. The above was indeed observed as it was noticed during the experiments that to compensate for the small changes in the resistance between the probe plates as a consequence of daily variations of the resistivity of the tap water, the accidental bangings of the probe, and the accumulations of grease and dirt on the surface of the plates, the knob controlling R_p had to be adjusted over quite a wide range.

The sensitivity of R_{xp} and R_{yp} to changes in R_x and R_y caused the instrument to give different signal outputs for the same frazil ice concentration. It is seen from Fig. 4 that the instrument measures the changes in R_{ex} and R_{ex} is given by the first equation of Equation (51). The differentiation of that equation with respect to frazil ice concentration c gives

$$\frac{dR_{ex}}{dc} = \frac{1}{(1 + R_x/R_{xp})^2} \frac{dR_x}{dc} \qquad \ldots \ldots \ldots \ldots (58)$$

The above equation shows that the change in R_{ex} not only depends on the change in R_x alone, but on the ratio R_x/R_{xp} also. Since R_{xp} is capable of wide variation while R_x changes little, the correlation between the signal output and the frazil ice concentration therefore can be highly different from test to test.

Understanding the above, the instrument can be made to give a better signal output/frazil concentration correlation by using variable

resistances connected in series with R_x and R_y for fine adjustment of the bridge instead of the present design.

The high value of the median of the measured concentration to calculated concentration ratio of 3.31 presents a pleasing but unexplainable puzzle at this point. Although the small resistivity of the tested water created a corrective factor of 1.35 for the present tests, it can be shown that the corrective factor can at the most reach a value of 1.8 and that happens when the resistivity of the tested water become negligible. With a corrective factor of 1.8, the median value of c_i/c_t of 3.31 is modified to 2.48, which is still a high value.

The shape and the finite size of the ice crystals may be the other factors responsible for the magnified effect of frazil ice on the resistance of the tested water. By approximately considering a frazil ice crystal as an elongated spheroid with a length to breadth ratio of 10:1, Appendix shows that the resistance effect based on fractional displacement theory should be increased by a multiplying factor of 1.65. However, even with this factor taken into account, the median value of c_i/c_t would still be 2.0. Further theoretical investigation of the causes of the high c_i/c_t ratio is beyond the scope of this report. However, the magnified effect of frazil ice on water resistance is a welcome one because it will make the instrument more sensitive and the hardware design will be easier.

The equation relating the signal output of the sensing resistance bridge and the concentration of frazil ice, Equation (34), may be rewritten as:

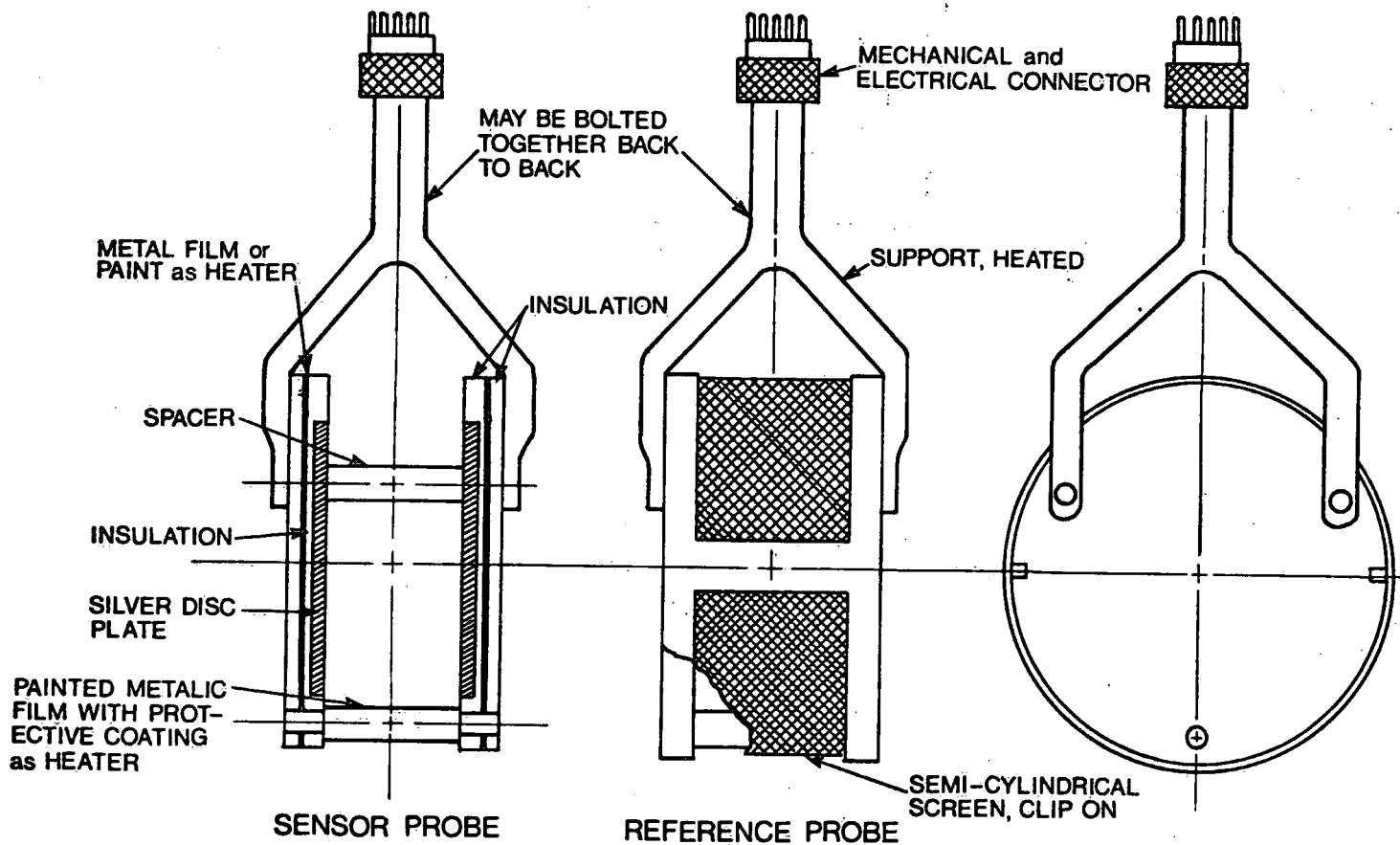$$\Delta = \frac{- N_*}{(1 + N_*)^2} \, c \tag{59}$$

where

$$N_* = \frac{R_y'}{R_1}$$

(60)

For the experimental instrument, because the values of N_* were different between calibration and the test conditions, the measured concentrations had to be corrected. To eliminate the necessity of measuring the resistance of the ice-free water between the probe plates (R_y) and the correction process, the instrument should be so designed that N_* is a constant, preferably equal to unity.

Fig. 7 shows the circuitry that gives $N_* = 1$. Part a of the diagram shows three resistance bridges which demonstrate how step by step $N_* = 1$ is obtained. The first bridge is for adjusting R_1 to be equal to R_y. After $R_1 = R_y$ is obtained, the substitution of R_y by R_2 as shown by the second bridge and the subsequent adjustment gives $R_1 = R_2 = R_y$. The use of $R_1 = R_2 = R_y$ in the third bridge gives the sensing bridge of the instrument with $N_* = 1$. Fig. 7b is the circuit that comprises the above three bridges. By switching the switches to positions 1, 2 and 3, as indicated, the 3 bridges shown on part (a) will be formed. The design shown on Fig. 7 has the advantage that it enables the calibration (or zeroing) of the instrument under working condition.

The experimental probe reported here is far from satisfactory. The probe plates were rectangular so were hard to be made identical. The outside of the side plates was exposed to the ambient fluid and the stray of the electric lines from the edges and corners was excessive. In addition, the probe was unnecessarily bulky and structurally weak. The redesign of the probe therefore, is necessary. To measure frazil ice under different conditions, different probes are needed. Fig. 8 shows the conceptual design of two probes. Probe A is for measuring frazil ice in waters where turbul-

a: Probe For Water With Low Mean Velocities

MECHANICAL and ELECTRICAL CONNECTOR

MAY BE BOLTED TOGETHER BACK TO BACK

METAL FILM or PAINT as HEATER

INSULATION

SUPPORT, HEATED

SPACER

INSULATION

SILVER DISC PLATE

PAINTED METALIC FILM WITH PROTECTIVE COATING as HEATER

SEMI-CYLINDRICAL SCREEN, CLIP ON

SENSOR PROBE   REFERENCE PROBE

NOTE: Reference probe identical with sensor probe except with screens added. Electrical connections not shown.

b: Probe For Flowing Water

REFERENCE PROBE, with CONE:
SENSOR PROBE, without CONE:

SILVER

FLOW

Same kind of heating provision as in 'a' not shown.
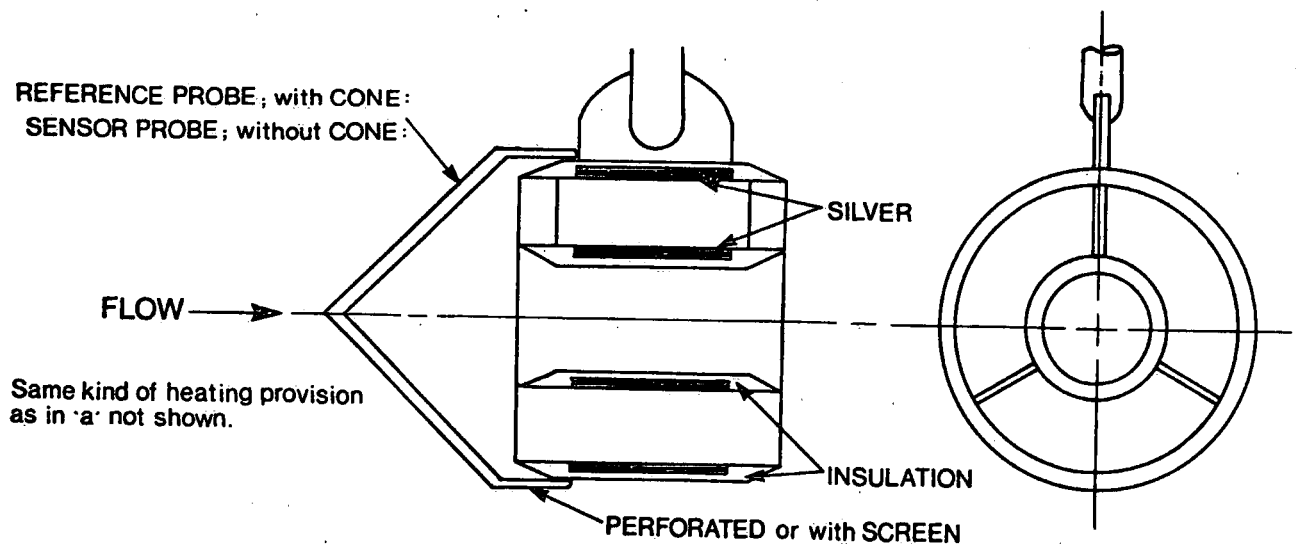
INSULATION

PERFORATED or with SCREEN

Figure 8   CONCEPTUAL DESIGN OF IMPROVED PROBES

ence is mainly induced by surface waves or agitations and probe B is for

frazil ice sensing when a noticeable mean flow is present. It is recom-

mended that in phase II of the instrument development, probes should be

constructed according to Fig. 8. *What is effect of anchor ice formation on the probes?*

Although it has been shown that theoretically an instrument

built on the capacitance sensing principle has the advantage of having

$M = 1$, or that the measurement is not affected by the source of water,

the hardward design of such an instrument has problems of its own. The

problems arise because the small capacitance involved. For scientific

usage of the instrument, it is desirable that the sampled volume is approxi-

mately cubic. Under such a situation the area to separation ratio of the

probe plates A/S is approximately equal to S. The substitution of this value

of A/S into Equation (10) with $\varepsilon_{H_2O} = 80 \times \dfrac{1}{36\Pi} \times 10^{-9}$ Farad/m gives the

capacitance of the reference probe to be $C_y \simeq S \times 10^{-9}$ Farad. Even with

a huge plate separation of $S = 1$ m, the capacitance one has to deal with

is still only 10^{-9} Farad, a very small capacitance to handle. The problem

of building a capacitance instrument thus becomes a technological feasi-

bility problem.

CONCLUSIONS

At the conclusion of Phase I of the instrument development, one
may say that scientifically the quantitative measurement of frazil ice
concentration by sending the effect of frazil ice on the resistivity
or on the dielectric constant of water is possible. Theoretical in-
vestigations show that a capacitance instrument appears to have a
certain advantage over a resistance instrument. However, the building
of a capacitance instrument is constrained by the small capacitance involved
that one must successfully handle. The problem thus becomes a technological
one. An experimental instrument based on the resistance principle has
been built and tested. The experimental instrument showed high promises.
Further development of the instrument should produce a manufacturable
prototype.

The unexpectedly high effect of frazil ice on the resistivity
of water needs more investigation. However, this does not affect the
development of the instrument if an instrument is to be calibrated before
it is used. The unexpected high sensitivity of resistance of water ice
presence comes as a welcome surprise because it increases the sensitivity
of the instrument.

Because of the clustering of frazil ice crystals, the cali-
bration of an instrument will always be a problem. A better calibration
technique than the one shown here will be very desirable.

ACKNOWLEDGEMENT

REFERENCES

Gilfilian, R.E., Line, W.L. and Osterkamp,T., Ice formation in a small
Alaskan Stream, UNESCO-5: Properties and Process of River
and Lake Ice, 1972.

Kristinsson, B. Ice Monitoring Equipment, Proc. IAHR, Symposium on Ice
and its action on hydraulic structures, Reyjavik, Sept. 1970,
pp. 1.1, 1-14.

Schmidt, C.C. and Glover, J.R. A frazil ice concentration measuring system
using a laser doppler velocimeter, Journ, of Hydraulic Research,
IAHR, Vol. 13, No. 3, 1975, pp. 299-314.

Stratton, J.A. Electromagnetic Theory, McGraw-Hill, 1941.

Tsang, G. Conceptual design of a multi-purpose instrument for winter stream
metering, Proc. Int. Symp. on Advanced Concepts and Techniques in
the study of Snow and Ice Resources, Monterey, Dec., 1973. Pub-
lished by the U.S. National Academy of Sciences, 1974, pp. 688-698.

In the theoretical development part of the report, the fractional displacement theory that the presence of frazil reduces proportionally the number of ions in the volume between the probe plates and the conductive area of the plates was used, and from this theory Eq.(8)

$$\frac{R_x}{R_y} = \frac{1}{1-c} = 1 + c \qquad \ldots\ldots\ldots\ldots \text{(A1)}$$

and Eq. (21)

$$\rho_0 = (1 - \overline{c}) \rho_{H_2O} \qquad \ldots\ldots\ldots\ldots \text{(A2)}$$

were obtained. The extension of the fractional displacement theory to the dielectric constant of the medium gave Eq. (11)

$$\varepsilon_x = (1 - c) \varepsilon_{H_2O} + c \varepsilon_{ice} \qquad \ldots\ldots\ldots\ldots \text{(A3)}$$

Equations (A1) and (A2) are only true under two specific conditions. The first is that the ice praticles are very small that they do not affect the electric line between the plates, and the second is that the ice forms long rods extending from one plate to the other and in so doing proportionally reduces the conductive area of the plates. For Eq. (A3), it only holds under the second condition. For frazil ice, since the ice crystals are finite in size and distribute randomly in space, both in quantity and orien-

---

tation, neither of the above conditions are satisfied and Equations (A1)
to (A3) thus are not really valid. This probably is one of the reasons
for the larger measured values of frazil ice concentration than the theo-
retically predicted values.

For better mathematical expressions for later comparisons, con-
ductivity τ will be used in place of resistivity. With the fractional
displacement theory, the change in conductivity of the medium following
the formation of frazil ice is given by

$$\Delta\tau \quad = \quad - c\tau \qquad \ldots \ldots \ldots \ldots \text{(A4)}$$

Because the presence of the randomly distributed and oriented frazil ice
crystals causes the diversion of the electric lines, the reduction in
conductivity will be more than that shown by the above equation and to
account for this, a multiplying factor m_τ greater than unity, may be used
to change the above equation to

$$\Delta\tau \quad = \quad - m_\tau \, c\tau \qquad \ldots \ldots \ldots \ldots \text{(A5)}$$

Equation (A3) gives the dielectric constant of the frazil ice-laden water.
The change in dielectric constant from the ice-free condition to the ice-
laden condition may be obtained from it to be

$$\Delta\varepsilon \quad = \quad - \varepsilon_{H_2O} \, (1 - \gamma_\varepsilon) \, c \qquad \ldots \ldots \ldots \ldots \text{(A6)}$$

where $\gamma_\varepsilon = \varepsilon_{ice}/\varepsilon_{H_2O}$, as has been defined earlier in the text. Similar

to the conductivity case, another multiplying factor m_ϵ may be introduced to take into account the diversion of the dielectric field line and Equation (A6) becomes

$$\Delta\epsilon \quad = \quad - m_\epsilon \ \epsilon_{H_2O} \ (1-\gamma_\epsilon) \ c \qquad \ldots \ldots \ldots \ldots \quad (A7)$$

It may be pointed out that m_τ and m_ϵ are different because while physically frazil ice may be considered as an insulator that the electric lines cannot penetrate into, it may not be considered as impermeable to dielectric field lines because it has a fine, though small, relative dielectric constant (5/80) with respect to water.

To evaluate m_ϵ, the polarization theory may be used. According to the theory, for water with suspended frazil ice particles, the polarization induced by an electric field $\vec{E}$ is given by

$$\vec{P} \quad = \quad n\alpha \ \epsilon_{H_2O} \ \vec{E} \qquad \ldots \ldots \ldots \ldots \quad (A8)$$

where n is the number of ice crystals per unit volume and α is the polarizability of an ice particle. In the above equation, $\vec{E}$ is the field including the applied field and the field from the dipoles produced by the applied field. For low ice concentrations, which generally is the case, $\vec{E}$ may be approximately considered as equal to the applied field.

From the definition of displacement flux density, one sees that the displacement flux density between the probe plates is given by

$$\vec{D} \quad = \quad \epsilon_{H_2O} \ \vec{E} + \vec{P} \quad = \quad \epsilon_{H_2O} \ (1 + n\alpha) \ \vec{E} \qquad \ldots \ldots \quad (A9)$$

By definition one also has

$$\vec{D} \quad = \quad \varepsilon_{med} \, \vec{E} \qquad \cdots \cdots \cdots \cdots \cdots \quad (A10)$$

where ε_{med} is the dielectric constant of the water and frazil ice mixture.
From the above two equations, one has

$$\Delta \varepsilon \quad = \quad \varepsilon_{med} - \varepsilon_{H_2O} \quad = \quad \varepsilon_{H_2O} \, n\alpha \qquad \cdots \cdots \cdots \cdots \quad (A11)$$

which is the change in dielectric constant as the water between the probe
plates changes from ice-free to ice-laden. From Equations (A7) and (A11)
one has

$$m_\varepsilon \quad = \quad - \frac{n\alpha}{(1 - \gamma_\varepsilon)c} \quad = \quad - \frac{\alpha}{(1 - \gamma_\varepsilon)V_p} \qquad \cdots \cdots \cdots \quad (A12)$$

where $V_p = c/n$ is the volume of an (average) ice crystal.

The polarizability or electric susceptibility α of an ice crystal
is a function of its orientation and shape and the dielectric constant ratio
γ_ε. If frazil ice crystals can be considered as ellipsoidal particles (In
fact, frazil ice crystals are of needle form as shown on Plate 4), Stratton
(1941) showed that if the electric field is parallel to one of its principal
axes, the polarizability is given by

$$\alpha_i \quad = \quad \frac{V_p}{L_i + \dfrac{1}{(\gamma_\varepsilon - 1)}} \qquad \cdots \cdots \cdots \cdots \cdots \quad (A13)$$

where the subscript i indicates one of the principal axes, and L_i is given by

$$L_i = \frac{\ell_1 \ell_2 \ell_3}{2} \int_0^\infty (s + \ell_i^2)^{-1} \left[(s+\ell_1^2)(s+\ell_2^2)(s+\ell_3^2) \right]^{\frac{1}{2}} ds$$

$$\dots \dots \dots \dots \text{(A14)}$$

where ℓ_1, ℓ_2 and ℓ_3 are the three dimensions along the principal axes. Since the orientation of the frazil ice crystals is random, one may simplify the matter by considering that one-third of all the crystals has its first principal axis, another third has its second principal axis, and the last third with its third principal axis aligned with the applied electric field. With such a simplification, the average polarizability of the ice crystals in mass is given by

$$\alpha = \frac{\alpha_1 + \alpha_2 + \alpha_3}{3} \qquad \dots \dots \dots \dots \text{(A15)}$$

With Equations (A12) to (A15), the multiplying factor m_ε is calculated for a few spheroid cases and shown on Table 2.

The multiplying factor m_τ for conductivity may also be obtained by a similar method from Equations (A5) and the definition equation for conductivity

$$\vec{J} = \tau \vec{E} \qquad \dots \dots \dots \dots \text{(A16)}$$

where $\vec{J}$ is the current density. However, a comparison of the above equation with Equation (A10) shows that these two equations are identical so any solution obtained for dielectric constant can be directly applied to conductivity. A comparison between Equations (A5) and (A6) shows that if $\gamma_\varepsilon = 0$, the two equations will be of exactly the same form. Thus, according to the above, by assigning $\gamma_\varepsilon = 0$, the multiplying factor m_τ may also be

TABLE 2. Multiplying factors m_ϵ and m_τ for some spheroids

Case	ℓ_1	ℓ_2	ℓ_3	m_ϵ	m_τ
Sphere	1	1	1	1.45	1.50
Prolate spheroid	10	1	1	1.57	1.65
Very long spheroid	∞	1	1	1.59	1.67
Oblate spheroid	1	5	5	1.88	2.09
Flat spheroid	1	10	10	2.44	3.02
Thin disc	1	∞	∞	6.00	∞

Note: 1. The volume of the spheroid is immaterial as V_p disappears from the final relationship by cancelling.
2. The electric field is in the ℓ_1 direction.

calculated from Equations (A12) to (A15). The calculated values of m_τ for different spheroid cases are also shown on Table 2.

Table 2 shows that m_ε and m_τ have the least value for a sphere. The elongation and the compression of the sphere both increase the values of m_ε and m_τ. It is seen from Plate 4 that frazil ice crystals may be approximately considered as prolate spheroids with dimensions $\ell_1 : \ell_2 : \ell_3 = 10 : 1 : 1$ and thus give a conductivity multiplying factor of $m_\tau = 1.65$. The use of this multiplying factor in the experimental results changes the median value of the c_i/c_t ratio from 3.31 to 2.00. The measured frazil ice concentration is still twice the calculated concentration.

0029533E

TSANG, Gee.